87.00

Ontario

Ontario Geological Survey
Open File Report 6105

The Neoarchean Rice Lake Batholith and its Place in the Tectonomagmatic Evolution of the Swayze and Abitibi Granite-Greenstone Belts, Northeastern Ontario

2003

Ontario

ONTARIO GEOLOGICAL SURVEY

Open File Report 6105

The Neoarchean Rice Lake Batholith and its Place in the Tectonomagmatic Evolution of the Swayze and Abitibi Granite-Greenstone Belts, Northeastern Ontario

by

J.K. Becker and K. Benn

2003

Parts of this publication may be quoted if credit is given. It is recommended that reference to this publication be made in the following form:

Becker, J.K. and Benn, K. 2003. The Neoarchean Rice Lake batholith and its place in the tectonomagmatic evolution of the Swayze and Abitibi granite-greenstone belts, northeastern Ontario; Ontario Geological Survey, Open File Report 6105, 42p.

© Queen's Printer for Ontario, 2003

© THE QUEEN'S PRINTER FOR ONTARIO
2003

REPRODUCED WITH PERMISSION

L'IMPRIMEUR DE LA REINE POUR L'ONTARIO
2003

REPRODUIT AVEC PERMISSION

Micromedia
ProQuest

20 Victoria Street
Toronto, Ontario M5C 2N8
tel: (416) 362-5211
toll free: 1-800-387-2689
fax: (416) 362-6161
web: www.micromedia.ca

87.00

Ontario

Ontario Geological Survey
Open File Report 6105

The Neoarchean Rice Lake Batholith and its Place in the Tectonomagmatic Evolution of the Swayze and Abitibi Granite-Greenstone Belts, Northeastern Ontario

2003

Ontario

ONTARIO GEOLOGICAL SURVEY

Open File Report 6105

The Neoarchean Rice Lake Batholith and its Place in the Tectonomagmatic Evolution of the Swayze and Abitibi Granite-Greenstone Belts, Northeastern Ontario

by

J.K. Becker and K. Benn

2003

Parts of this publication may be quoted if credit is given. It is recommended that reference to this publication be made in the following form:

Becker, J.K. and Benn, K. 2003. The Neoarchean Rice Lake batholith and its place in the tectonomagmatic evolution of the Swayze and Abitibi granite-greenstone belts, northeastern Ontario; Ontario Geological Survey, Open File Report 6105, 42p.

© Queen's Printer for Ontario, 2003

© Queen's Printer for Ontario, 2003.

Open File Reports of the Ontario Geological Survey are available for viewing at the Mines Library in Sudbury, at the Mines and Minerals Information Centre in Toronto, and at the regional Mines and Minerals office whose district includes the area covered by the report (see below).

Copies can be purchased at Publication Sales and the office whose district includes the area covered by the report. Although a particular report may not be in stock at locations other than the Publication Sales office in Sudbury, they can generally be obtained within 3 working days. All telephone, fax, mail and e-mail orders should be directed to the Publication Sales office in Sudbury. Use of VISA or MasterCard ensures the fastest possible service. Cheques or money orders should be made payable to the *Minister of Finance.*

Mines and Minerals Information Centre (MMIC) Macdonald Block, Room M2-17 900 Bay St. Toronto, Ontario M7A 1C3	Tel:	(416) 314-3800
Mines Library 933 Ramsey Lake Road, Level A3 Sudbury, Ontario P3E 6B5	Tel:	(705) 670-5615
Publication Sales 933 Ramsey Lake Rd., Level A3 Sudbury, Ontario P3E 6B5	Tel: Fax: E-mail:	(705) 670-5691(local) 1-888-415-9845(toll-free) (705) 670-5770 pubsales@ndm.gov.on.ca

Regional Mines and Minerals Offices:

Kenora - Suite 104, 810 Robertson St., Kenora P9N 4J2

Kirkland Lake - 10 Government Rd. E., Kirkland Lake P2N 1A8

Red Lake - Box 324, Ontario Government Building, Red Lake P0V 2M0

Sault Ste. Marie - 70 Foster Dr., Ste. 200, Sault Ste. Marie P6A 6V8

Southern Ontario - P.O. Bag Service 43, 126 Old Troy Rd., Tweed K0K 3J0

Sudbury - Level B3, 933 Ramsey Lake Rd., Sudbury P3E 6B5

Thunder Bay - Suite B002, 435 James St. S., Thunder Bay P7E 6S7

Timmins - Ontario Government Complex, P.O. Bag 3060, Hwy. 101 East, South Porcupine P0N 1H0

Toronto - MMIC, Macdonald Block, Room M2-17, 900 Bay St., Toronto M7A 1C3

This report has not received a technical edit. Discrepancies may occur for which the Ontario Ministry of Northern Development and Mines does not assume any liability. Source references are included in the report and users are urged to verify critical information. Recommendations and statements of opinions expressed are those of the author or authors and are not to be construed as statements of government policy.

If you wish to reproduce any of the text, tables or illustrations in this report, please write for permission to the Team Leader, Publication Services, Ministry of Northern Development and Mines, 933 Ramsey Lake Road, Level B4, Sudbury, Ontario P3E 6B5.

Cette publication est disponible en anglais seulement.

Parts of this report may be quoted if credit is given. It is recommended that reference be made in the following form:

Becker, J.K. and Benn, K. 2003. The Neoarchean Rice Lake batholith and its place in the tectonomagmatic evolution of the Swayze and Abitibi granite-greenstone belts, northeastern Ontario; Ontario Geological Survey, Open File Report 6105, 42p.

Contents

Abstract ix

Introduction 1

Swayze Greenstone Belt 3
- Stratigraphy 5
- Stratigraphic Correlations of the Swayze and Abitibi Greenstone Belts 7
- Foliation in the Swayze Greenstone Belt 11
- Orientation of Bedding in the Swayze Greenstone Belt 11
- Deformation 13

Rice Lake Batholith 15
- Introduction 15
- Granitoid Rocks of the Rice Lake Batholith 15
- Age Relationship 15
- Geochemistry 16
- Macroscopic Foliation of the Rice Lake Batholith 17
- Petrography 19
- Magnetic Measurements of Granitoid Rocks 25
  - Introduction 25
  - Magnetic Properties 25
  - Magnetic Foliation 27
  - Magnetic Lineation 29
- Deformations of the Rice Lake Batholith 31

Summary 32
- Swayze and Abitibi Greenstone Belts 32
- Rice Lake Batholith 32
- Implications for the Regional Development of the Swayze and Abitibi Greenstone Belts 34

Acknowledgments 35

Appendix 1. Data from the AMS Measurements 36

References 40

Metric Conversion Table 42

FIGURES

1. Simplified geological map of the southwestern Abitibi Subprovince, including the Swayze and Abitibi granite-greenstone belts. The Kenogamissi batholith is situated between the Swayze greenstone belt in the west and the Abitibi greenstone belt in the east. This study concentrates on the Neoarchean intrusion of the Rice Lake batholith in the southwestern lobe of the Kenogamissi batholith. 1

2. Geological map of the Swayze greenstone belt. The distribution of lithological units within the Swayze greenstone belt is controlled by the east-west trending folds. 2

3. Top indicators in a) pillow lavas of the Trailbreaker group (shelves) and in b) greywackes of the Ridout group (cross-bedding). 5

4. Geological map of the Abitibi greenstone belt with its respective lithotectonic assemblages 6
5. The Opeepeesway conglomerates display many similarities with conglomerates in the Timiskaming assemblage of the Abitibi greenstone belt. A) Cobbles in the conglomerates are approximately 5 to 10 cm long. B) The so-called "red chert" clasts in the Opeepeesway conglomerates..... 8
6. Orientation of bedding planes in the Opeepeesway area of the Swayze greenstone belt..... 9
7. Map of the macroscopic foliation traces in the Swayze greenstone belt..... 10
8. Schmidt net projections of the macroscopic foliation in the Swayze greenstone belt..... 11
9. Orientation of bedding in the Swayze greenstone belt..... 12
10. Macroscopic evidence for north-south trending folds. A) North-south trending folds in the iron formations that cap the Woman River formation of the Marion group. B) North-south trending fold in greywackes of the Trailbreaker group..... 13
11. General geology of the Rice Lake batholith (southwestern lobe of the Kenogamissi batholith). 14
12. Crosscutting relationships and xenoliths in the Rice Lake batholith. 16
13. A) Total alkali versus silica diagram. B) AFM diagram 16
14. A) Y versus Nb diagram, B) (Y+Nb) versus Rb diagram, and C) geodynamic setting. 17
15. Traces of the macroscopic foliation in the Rice Lake batholith. 18
16. Location map of thin sections and outcrops shown in Figures 17, 18 and 19 and described in the text 20
17. Thin sections of hornblende diorite from the northern margin (JB199, *see* Figure 16 for location). A) parallel to the foliation, B) parallel to the lineation/perpendicular to the foliation and C) perpendicular to the foliation and lineation..... 21
18. All sample locations are shown in Figure 16. A) Granitoid rocks with gneissic texture from within the Ridout high-strain zone at the southern margin of Rice Lake batholith. B) Granitoid rocks of the hornblende diorite at the northern margin of Rice Lake batholith. C) Thin section of the biotite granodiorite. No strong submagmatic or solid-state deformations can be observed. D) Thin section of a hornblende diorite sample with a strong metamorphic overprint from near the centre of Rice Lake batholith. 22
19. Thin sections of hornblende tonalite from the southern margin (JB100, *see* Figure 16 for location). A) parallel to the foliation, B) parallel to the lineation/perpendicular to the foliation and C) perpendicular to the foliation and lineation..... 23
20. A) Representation of the three main magnetic axes and their bulk values through the so-called magnetic ellipsoid. B) Since all of the calculated parameters used in this study depend on the ratio of the value of the different main magnetic axes, they show a mathematical dependence 24
21. Susceptibility diagrams for the three main units of the Rice Lake batholith. 26
22. Traces of the magnetic foliation in the three main units of the Rice Lake batholith. 28
23. Schmidt net projections of the magnetic foliation (lower hemisphere): a) biotite granodiorite, b) hornblende tonalite and c) hornblende diorite. 29
24. Map of the magnetic lineation. 30
25. Schmidt net projections of the magnetic lineation (lower hemisphere): a) biotite granodiorite, b) hornblende tonalite and c) hornblende diorite. 31

TABLES

1. Comparison of the stratigraphy of the Swayze and Abitibi greenstone belts..... 4

103-04834/

Abstract

The Swayze and Abitibi greenstone belts have long been considered to represent two independent greenstone belts that are separated by the Kenogamissi batholith. This study concentrates on the southwestern part of the Kenogamissi batholith (Rice Lake batholith) and the surrounding supracrustal host rocks of the Swayze greenstone belt by comparing the Swayze and Abitibi greenstone belt and their relationship to the Kenogamissi batholith. The Abitibi greenstone belt has been extensively studied by geochemical, geochronological, structural and geophysical techniques that have been used to characterize the different lithotectonic units. In comparison, the Swayze greenstone belt was only studied at a regional scale until recently, when it has become the focus of more detailed studies.

For this project, detailed structural, geochemical and geochronological analyses, as well as magnetic measurements, have been performed which suggest that the two belts are closely related to each other. The different lithotectonic assemblages of the Abitibi greenstone belt show close temporal relationships with the metasedimentary and metavolcanic units in the Swayze greenstone belt, including the unconformities between the different groups and assemblages. Furthermore, the tectonic history is comparable between these two belts. Two major deformation events, generating two different sets of folds, have been documented in the Swayze greenstone belt as well as in the Abitibi greenstone belt.

The earlier folds trend north-south and, typically, they can be recognized from the orientation of the bedding planes. North-south trending folds were only documented in a small number of outcrops of metavolcanic rocks and iron formation, whereas the later, east-west oriented folds now dominate the outcrop pattern. Both these folding events have been recorded in the Rice Lake batholith and have also been verified using magnetic measurement techniques. The cross-folding resulted in the development of doubly plunging, east-west trending folds within the Rice Lake batholith. During the emplacement of the Rice Lake batholith, folding of the surrounding supracrustal rocks, against the rheologically more resistant granitoid rocks of the intrusion, resulted in development of a sinistral shear zone at the southern margin of the batholith that records flexural slip. At the northern margin of the Rice Lake batholith, supracrustal rocks are infolded between the Rice Lake batholith and the Kenogamissi batholith further to the north.

The geochemical analyses of some selected samples unambiguously show I-type granitoid magmas of volcanic-arc affinity.

The Neoarchean Rice Lake Batholith and its Place in the Tectonomagmatic Evolution of the Swayze and Abitibi Granite-Greenstone Belts

J.K. Becker[1] and K. Benn[2]
Ontario Geological Survey
Open File Report 6105
2003

---

[1] **Ottawa–Carleton Geoscience Centre and Department of Earth Sciences, University of Ottawa, Ottawa, Ontario K1N 6N5**
becker@jkbecker.de

[2] **Ottawa–Carleton Geoscience Centre and Department of Earth Sciences, University of Ottawa, Ottawa, Ontario K1N 6N5**
kbenn@uottawa.ca

Introduction

The Kenogamissi batholith is a very large granitoid complex situated at the boundary between the Swayze and Abitibi granite-greenstone belts (Figure 1). It is composed of several suites of poorly documented granitoid intrusions of different ages, as well as highly deformed, amphibolite-grade tonalitic to granodioritic gneisses. This study was initiated in 2000, primarily to document the internal structure of part of the Kenogamissi batholith, and to place it within the tectonomagmatic history of the Swayze and Abitibi greenstone belts. Structural mapping and sampling for microstructural, fabric, geochemical and geochronological analyses were carried out in the southwestern lobe of the Kenogamissi batholith, which is herein referred to as the Rice Lake batholith (*see* Figure 1). The name Rice Lake batholith is taken from one of the larger lakes that provides float plane access to the study area. The name refers to a Neoarchean granitoid massif of batholithic dimensions that is made up of diorite, tonalite and granodiorite. Also as part of this study, reconnaissance mapping was carried out in the supracrustal rocks of the Swayze greenstone belt that hosts the Rice Lake batholith, in order to compare the emplacement and deformation of the batholith to the regional deformational history.

Our field work relied heavily on recent maps of the Swayze greenstone belt and part of the Kenogamissi batholith that were produced by the Geological Survey of Canada (Heather and Shore 1999). The structural investigation of the Swayze greenstone belt for this study was performed in a reconnaissance fashion, and it was designed to check for evidence of more than one generation of regional folds and to verify possible unconformities. More detailed mapping and sampling was performed in the Rice Lake batholith. There, foliations, lineations and crosscutting intrusive relationships were

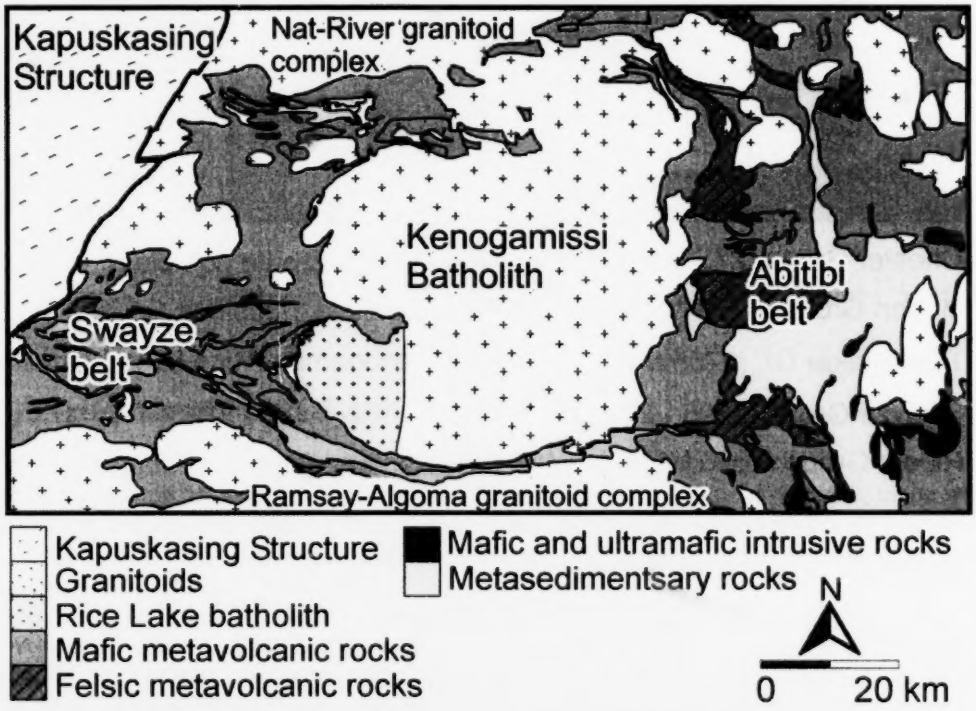

Figure 1. Simplified geological map of the southwestern Abitibi Subprovince, including the Swayze and Abitibi granite-greenstone belts. The Kenogamissi batholith is situated between the Swayze greenstone belt in the west and the Abitibi greenstone belt in the east. This study concentrates on the Neoarchean intrusion of the Rice Lake batholith in the southwestern lobe of the Kenogamissi batholith.

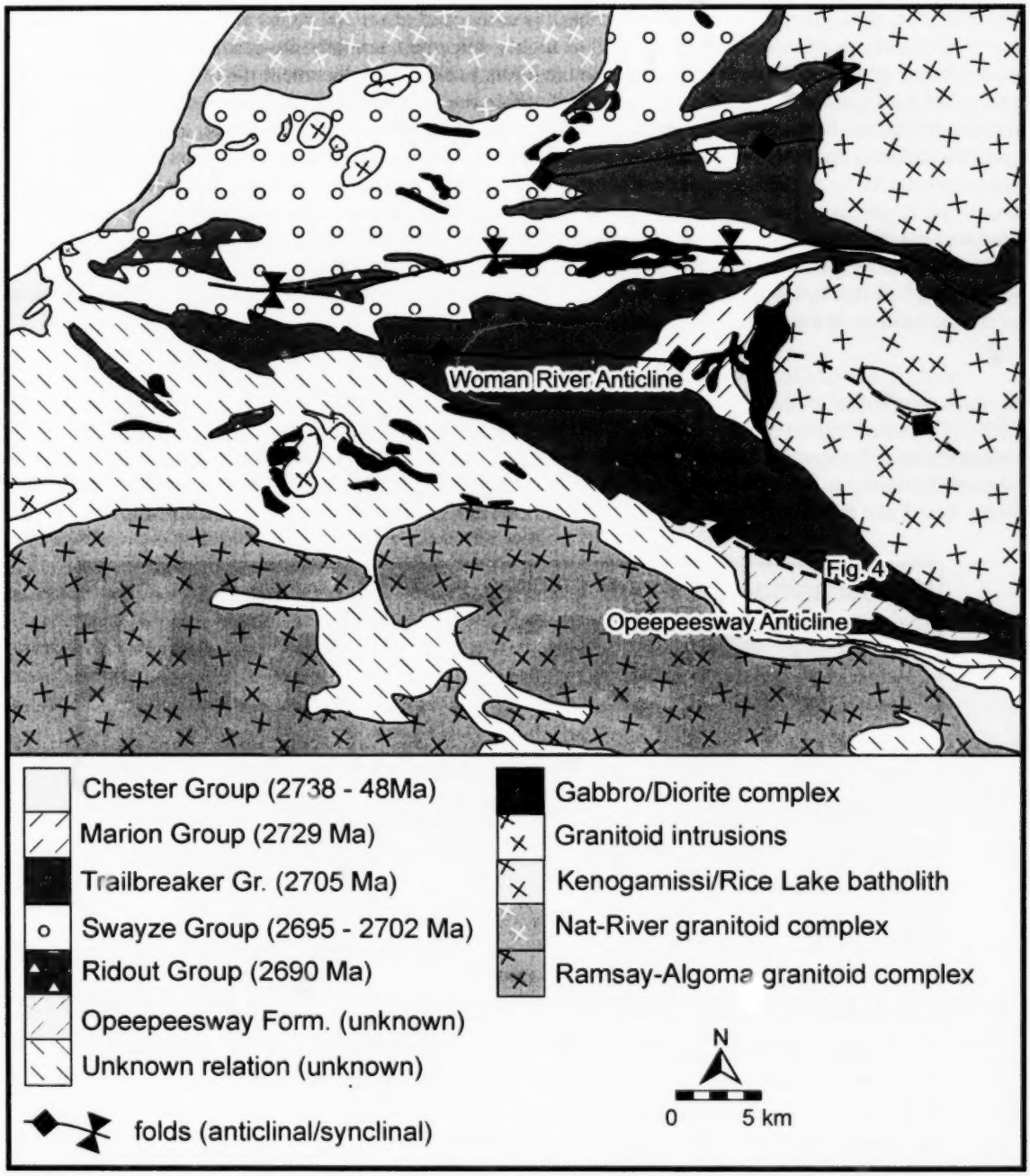

Figure 2. Geological map of the Swayze greenstone belt. The distribution of lithological units within the Swayze greenstone belt is controlled by the east-west trending folds.

documented and extensive sampling was carried out for petrographic studies and for measurements of the anisotropy of magnetic susceptibility (AMS) of the granitoids. The AMS data (Appendix 1) are of value because they give precise and reproducible measurements of the preferred orientations of the iron-rich minerals, providing a set of fabric data that is critical to interpretations of the intrusive and deformational history of the batholith.

In this report, we begin by reviewing the supracrustal lithologies that make up the Swayze greenstone belt and presenting the stratigraphic classification along with available geochronological data that help to bracket depositional ages. We then compare and contrast the stratigraphic records of the Swayze and Abitibi greenstone belts, highlighting similarities and differences. The idealized stratigraphic column of Ayer et al. (2002a) is used to represent the Abitibi. Ayer et al. (2002a) extended their stratigraphic classification to include the Swayze greenstone belt. In this report, we illustrate the stratigraphy of the Swayze greenstone belt using the earlier nomenclature of Heather (1998). We have chosen to use that previous stratigraphic classification because it allows us to mark the differences, as well as the similarities between the volcano-sedimentary and tectonic histories of the Swayze and Abitibi greenstone belts. Our mapping in the Swayze greenstone belt has led to a modification of the stratigraphic classification as the result of the documentation of a previously unrecognized unconformity, which indicates a very similar tectonic and sedimentary evolution for the Swayze and Abitibi greenstone belts, after 2687 million years ago.

. The structural geology of the Swayze greenstone belt is then presented, focussing on the evidence for the belt having undergone two periods of regional-scale folding, and the evidence for the previously unrecognized angular unconformity.

Our attention is then focussed on the Rice Lake batholith. The principal rock types are presented and crosscutting relationships are documented that demonstrate the relative ages of the three principal magmatic phases that make up the batholith. Some new geochemical data are presented and discussed for their significance in terms of the tectonic environment within which the magmas were generated. We then present our extensive structural and fabric database and discuss the emplacement and tectonic deformation of the granitoids. In the last section of the report, we briefly synthesize the data and draw conclusions regarding the significance of our results for our understanding of the tectonomagmatic evolution of the Swayze and Abitibi greenstone belts.

All supracrustal rocks have been metamorphosed to some extent and, thus, the prefix "meta" has been omitted for the sake of brevity.

Swayze Greenstone Belt

The Swayze greenstone belt is bounded in the north by the Nat River granitoid complex, to the west by the Kapuskasing uplift, to the south by the Ramsay–Algoma granitoid complex and to the east by the Kenogamissi batholith (*see* Figure 1). The volcanic and sedimentary rocks of the Swayze greenstone belt were previously classified into five stratigraphic groups (Heather and van Breemen 1994). From oldest to youngest, these are the Chester group, the Marion group, the Trailbreaker group, the Swayze group and the Ridout group (Figure 2; Table 1). Geochronological data for the different groups of the Swayze greenstone belt are not abundant and they are as yet insufficient to tightly constrain the absolute timing and duration of deposition for the different groups. Therefore, the geochronological data given below and in Table 1 are used to bracket, as closely as possible, the ages of the different units, while recognizing that further detailed geochronological work will undoubtedly help to refine our interpretations.

Table 1. Comparison of the stratigraphy of the Swayze and Abitibi greenstone belts. See text for further explanation. Abbreviation: St.-Rm., Stoughton–Roquemaure assemblage.

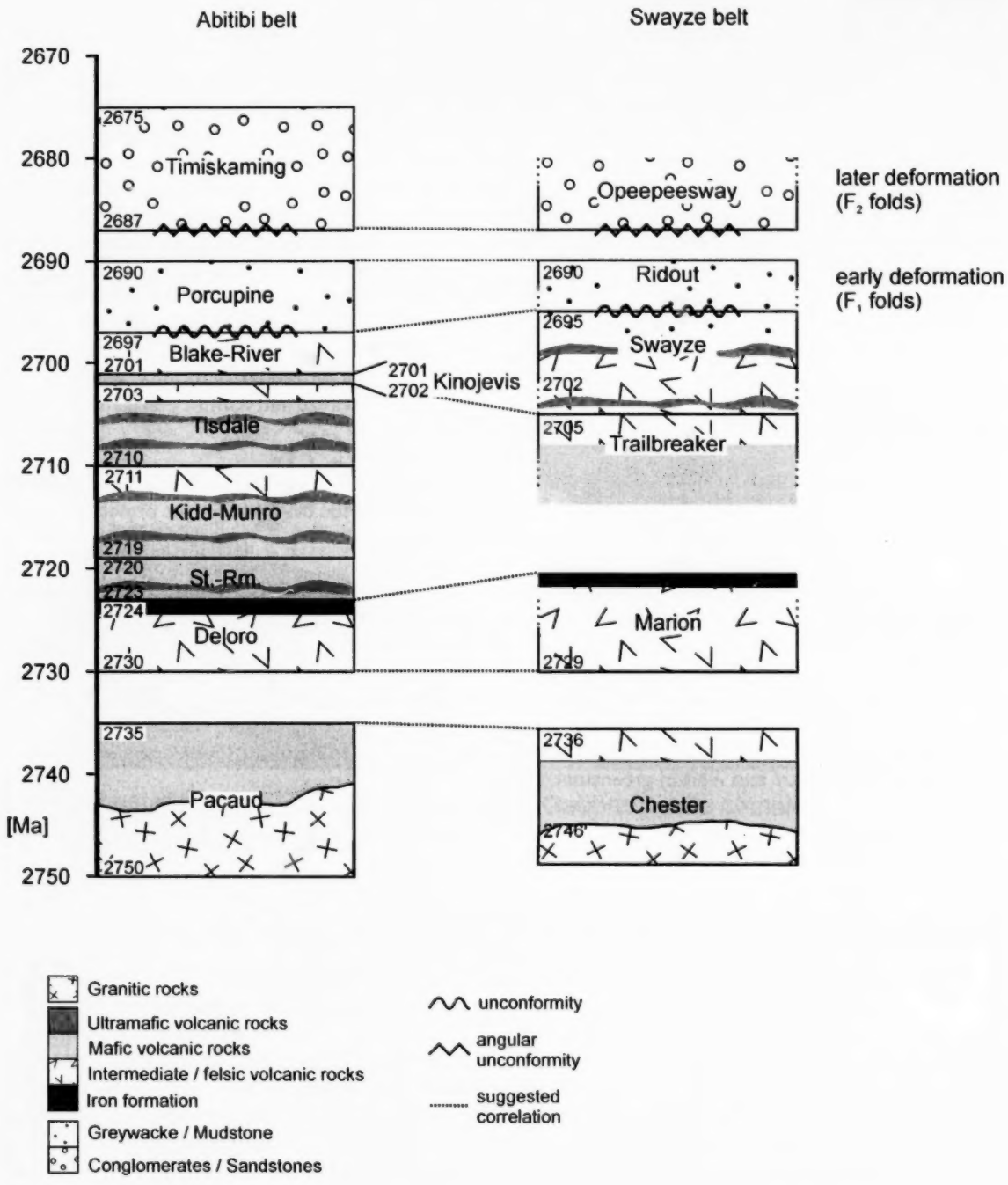

STRATIGRAPHY

The Chester group (2736 to 2746 Ma; Heather 1998) is the oldest stratigraphic group in the Swayze greenstone belt. It crops out mainly along the margins of large granitoid batholiths (e.g., Rice Lake batholith, *see* Figure 2), suggesting that lower parts of the volcano-sedimentary stratigraphy of the Swayze greenstone belt were dragged and/or stretched vertically along the margins of the batholiths as they were emplaced. The Chester group is composed of mafic volcanic rocks and amphibolites overlain by felsic to intermediate volcanic rocks, intercalated with chemical and clastic sedimentary rocks (*see* Table 1).

The Marion group consists of massive, calc-alkalic intermediate to felsic volcanic flows, ash and crystal tuffs interbedded with lapilli tuff and volcanic breccia. The Marion group is capped by iron formations. It crops out mainly within the Woman River anticline to the west of the Rice Lake batholith (*see* Figure 2). Ages of ca. 2729 Ma, obtained by U/Pb analyses of a quartz-eye bearing rhyolite breccia, are considered to be close to the beginning of the deposition of this group (Heather et al. 1996; Heather 1998).

The intermediate to felsic volcanic rocks of the Marion group are conformably overlain by a thick succession of massive, pillowed, Fe- to Mg-tholeiitic mafic volcanic rocks that represent the major part of the lower Trailbreaker group (Figure 3a). The upper part of the Trailbreaker group is made up of calc-alkalic, intermediate to felsic volcanic rocks, including pyroclastic, volcanoclastic and minor clastic sedimentary facies that are intruded by synvolcanic feldspar ± quartz porphyry dikes and stocks. A U/Pb zircon age of 2705±2 Ma from a quartz-phyric rhyolite of the Trailbreaker group (Heather and van Breemen 1994) is used in Table 1 as an approximate upper bracket for deposition of the Trailbreaker

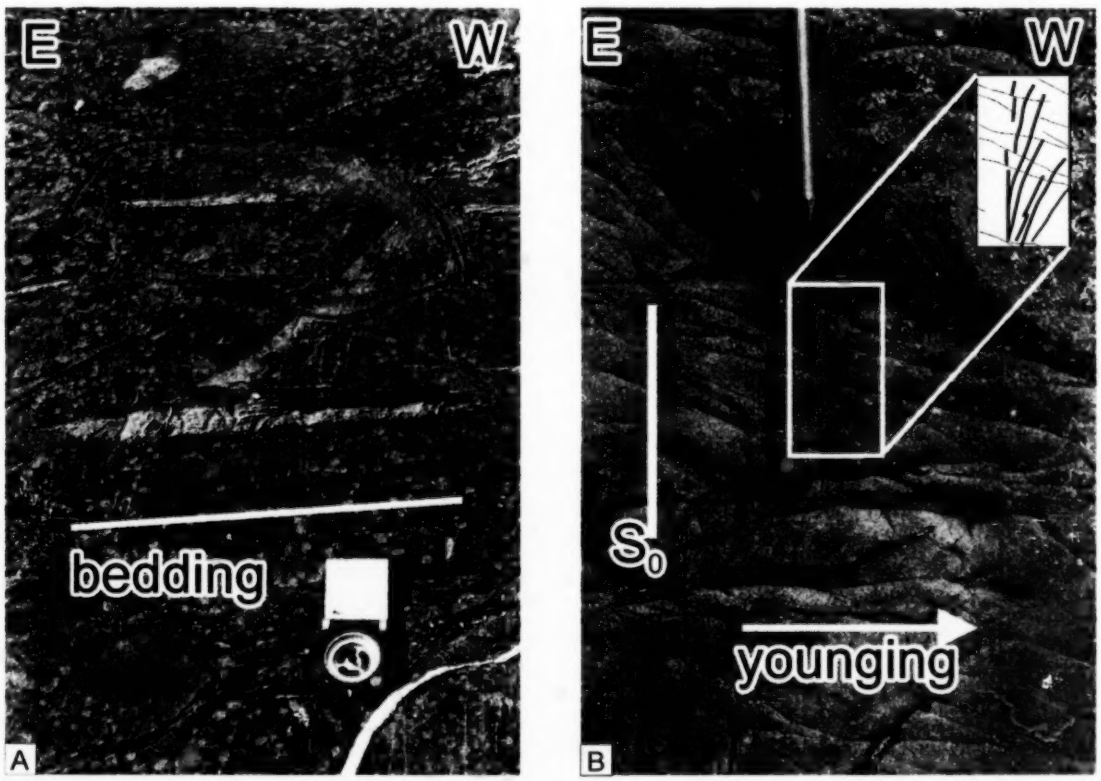

Figure 3. Top indicators in a) pillow lavas of the Trailbreaker group (shelves) and in b) greywackes of the Ridout group (cross-bedding).

group. The Trailbreaker group crops out along the northern and southern margins of the Rice Lake batholith and rocks of this group occupy a large part of the Woman River anticline, which is continuous almost as far as the Kapuskasing Structural Zone, to the west (*see* Figure 2).

The Swayze group occupies the largest area in the mapped parts of the Swayze greenstone belt (*see* Figure 2), however, outcrop is not abundant. The basal part of the Swayze group comprises pillowed Mg-tholeiites and basaltic komatiites intercalated with picritic komatiites. This succession exhibits well-developed hyaloclastic, variolitic and flow-top breccias. Komatiitic rocks are also common in the Swayze group. The overlying upper part of the Swayze group consists of felsic to intermediate pyroclastic and volcanoclastic rocks, interlayered with clastic sediments. The sedimentary rock mainly consists of intercalated quartz and/or feldspar-rich sandstones, siltstones, polymict conglomerates, wackes and mudstones. The absence of clasts of iron formation or granitoids in the conglomerates of the Swayze group distinguishes them from the conglomerates in the overlying Ridout group (see below). Ages determined for the Swayze group are 2697 Ma and 2695 Ma (Heather 1998) for felsic to intermediate volcanic rocks at the top of the Swayze group.

The Ridout group is the youngest stratigraphic group recognized by previous workers. Predominantly, it is made up of greywackes and conglomerates with minor amounts of feldspar ± quartz porphyry dikes and sheets. It has been proposed, based on "a map-scale discordance between the strike of the older rock units and the strike of the Ridout group..." (Heather 1998) that the Ridout group unconformably overlies all of the aforementioned groups (Heather 1998). A maximum depositional age of 2690 Ma for the Ridout group is based on the youngest ages obtained from zircons from a quartz-feldspar rich sandstone (Heather 1998).

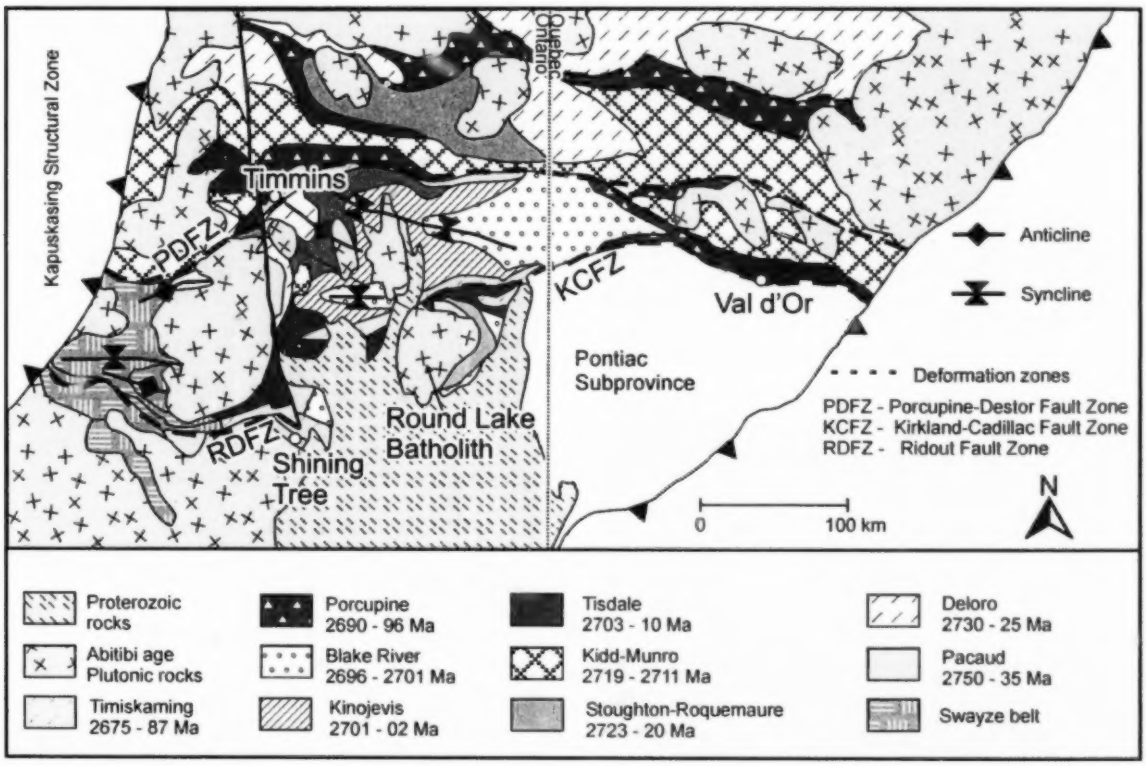

Figure 4. Geological map of the Abitibi greenstone belt with its respective lithotectonic assemblages according to Ayer et al. (2002a).

Previously, the Ridout group was thought to include the conglomerates and sandstones of the Opeepeesway formation. However, as we shall explain in "Stratigraphic correlations of the Swayze and Abitibi greenstone belts", an angular unconformity is now documented at the base of the Opeepeesway formation, which must, therefore, be broken out from the Ridout group (*see* Table 1). There are no geochronological data available for the Opeepeesway formation, but correlation with the Timiskaming assemblage in the Abitibi greenstone belt suggest the Opeepeesway sediments were deposited after 2679 million years ago (see next section).

STRATIGRAPHIC CORRELATIONS OF THE SWAYZE AND ABITIBI GREENSTONE BELTS

Based on previous mapping and geochronological studies of the Swayze greenstone belt (e.g., Heather et al. 1995) and on our own reconnaissance mapping, we are able to establish correlations between stratigraphic groups in the Swayze greenstone belt and the lithotectonic assemblages recognized in the Abitibi greenstone belt (Ayer et al. 2002a, 2002b; Figure 4). In the following, we will describe similarities and differences between the stratigraphic records in the Swayze and Abitibi greenstone belts, with reference to Table 1, and we will propose correlations between the volcanosedimentary histories of the two belts. The significance of the correlations will be discussed further in "Summary".

The oldest units of both belts, the Pacaud assemblage in the Abitibi belt and the Chester group in the Swayze belt, crop out mainly along the margins of large granitoid batholiths (compare Figures 2 and 4). This is consistent with the lower parts of the volcanosedimentary stratigraphy in both belts having been dragged up, or stretched vertically during emplacement of the granitoid intrusions. The Pacaud assemblage and the Chester group are both predominantly made up of mafic volcanic rocks. The Pacaud assemblage includes an important component of ultramafic volcanic rocks at its top, whereas the upper stratigraphic parts of the Chester group are intermediate to felsic rocks.

The Deloro assemblage and the Marion group consist of mafic to felsic rocks and, importantly, they are both capped by iron formations, which suggest similar depositional environments (*see* Table 1). Geochronological data from the Trailbreaker group in the Swayze greenstone belt suggest that this group may be correlated with the Tisdale assemblage of the Abitibi greenstone belt (*see* Table 1). The lithologies of the Trailbreaker group and the aforementioned assemblages in the Abitibi greenstone belt are readily comparable: tholeiitic volcanic rocks overlain by calc-alkalic intermediate to felsic rocks.

The Swayze group comprises pillowed Mg-tholeiitic basalts at its base that are overlain by intermediate to felsic volcanic rocks. The upper section of the Swayze group consists mainly of greywackes and sandstones with minor conglomerates. The published geochronological data for the Swayze group (2695 to 2703 Ma, *see* Table 1) indicates that it spans the same time as the Kinojevis and Blake River assemblages of the Abitibi greenstone belt. These assemblages comprise tholeiitic mafic volcanic flows at their base overlain by calc-alkalic volcanic rocks. An unconformity at the base of the Porcupine assemblage, reported in the Abitibi greenstone belt (e.g., Ayer et al. 2002b), may coincide with an unconformity between the Swayze and Ridout groups in the Swayze greenstone belt.

Heather (1998) assigned the Opeepeesway formation to the Ridout group in the Swayze greenstone belt. According to the published geochronological data (*see* Table 1), the Ridout group was deposited at the same time as the younger sediments of the Porcupine group. However, according to our observations, the Opeepeesway conglomerates bear very strong similarities to conglomerates in the Timiskaming assemblage. Highly flattened and stretched cobbles of granitoid composition are aligned in the foliation plane. The cobbles range in length from a few centimetres up to approximately 15 cm (Figure 5a).

Conglomerates of the Opeepeesway formation, as well as in the Timiskaming assemblage, can only be observed in morphological depressions (synclines); the granitoid cobbles may originate from the surrounding intrusions, which were eroded during rapid uplift and doming. Small (max. 5 cm long) fragments of red chert, the so-called red jasper which is typical of the Timiskaming assemblage, are common in outcrops of the Opeepeesway conglomerates (Figure 5b). Furthermore, in the Opeepeesway formation, an angular unconformity between the Opeepeesway conglomerates and the underlying greywackes can be demonstrated (Figure 6). On islands within Opeepeesway Lake, very weakly strained greywackes of the Ridout group strike north-south, and dip both to the east and west (*see* Figure 6). Younging direction indicators in the greywackes, such as cross-bedding (Figure 3b) and graded bedding, demonstrate that the beds are not overturned, and that they have been deformed by an upright and horizontal first-generation fold. There is no tectonic foliation associated with the fold in this region. In the overlying conglomerates of the Opeepeesway formation, on the north shore of Opeepeesway Lake and to the east and south of it, the bedding strikes east-west to northwest-southeast indicating the rock has been deformed by second-generation folds. These structural relations require the presence of an angular unconformity at the base of the Opeepeesway formation, which can, therefore, no longer be considered part of the Ridout group that underlies the angular unconformity. The angular unconformity between the conglomerates and the greywackes in the Opeepeesway formation shows that a revision of the previously

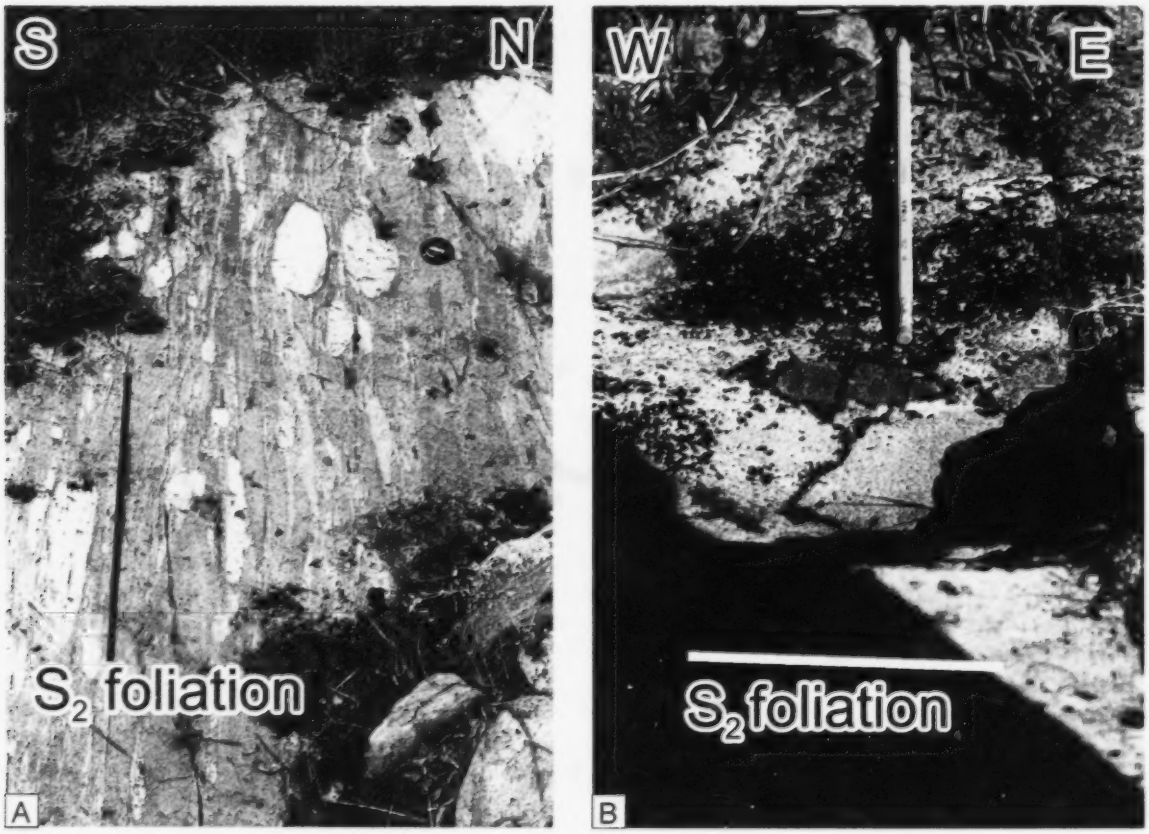

Figure 5. The Opeepeesway conglomerates display many similarities with conglomerates in the Timiskaming assemblage of the Abitibi greenstone belt. A) Cobbles in the conglomerates are approximately 5 to 10 cm long. B) The so-called "red chert" clasts in the Opeepeesway conglomerates. In the Timiskaming conglomerates, these red cherts are considered to be a distinctive feature of the Timiskaming conglomerates.

documented stratigraphy in the Swayze greenstone belt is necessary. The Opeepeesway formation can no longer be considered part of the Ridout group; we suggest that the deposition of at least the conglomerates in the Opeepeesway formation is coeval with the deposition of the Timiskaming assemblage and, therefore, must be younger than the Ridout group.

The most obvious difference between the Swayze and Abitibi greenstone belts is the relative abundance of komatiites in the Abitibi greenstone belt and their relative lack in the Swayze greenstone belt. In the Abitibi greenstone belt, komatiites have been described (e.g., Sproule et al. 2002) in the Pacaud, Stoughton–Roquemaure, Kidd–Munro and Tisdale assemblages, whereas, in the Swayze belt, komatiites have been observed only in the Swayze group (Heather et al. 1995) and in the Kidd–Munro assemblage in the northern part of the belt (Ayer et al. 2002a; Sproule et al. 2002). Komatiites are generated by a mantle plume and Sproule et al. (2002) relate the different occurrences of komatiites in the Abitibi greenstone belt to different depths of origin within a single mantle plume or to different mantle plumes. Geochemical analyses of the komatiites in the Swayze group indicate they are geochemically most similar to those of the Tisdale assemblage (Sproule et al. 2002).

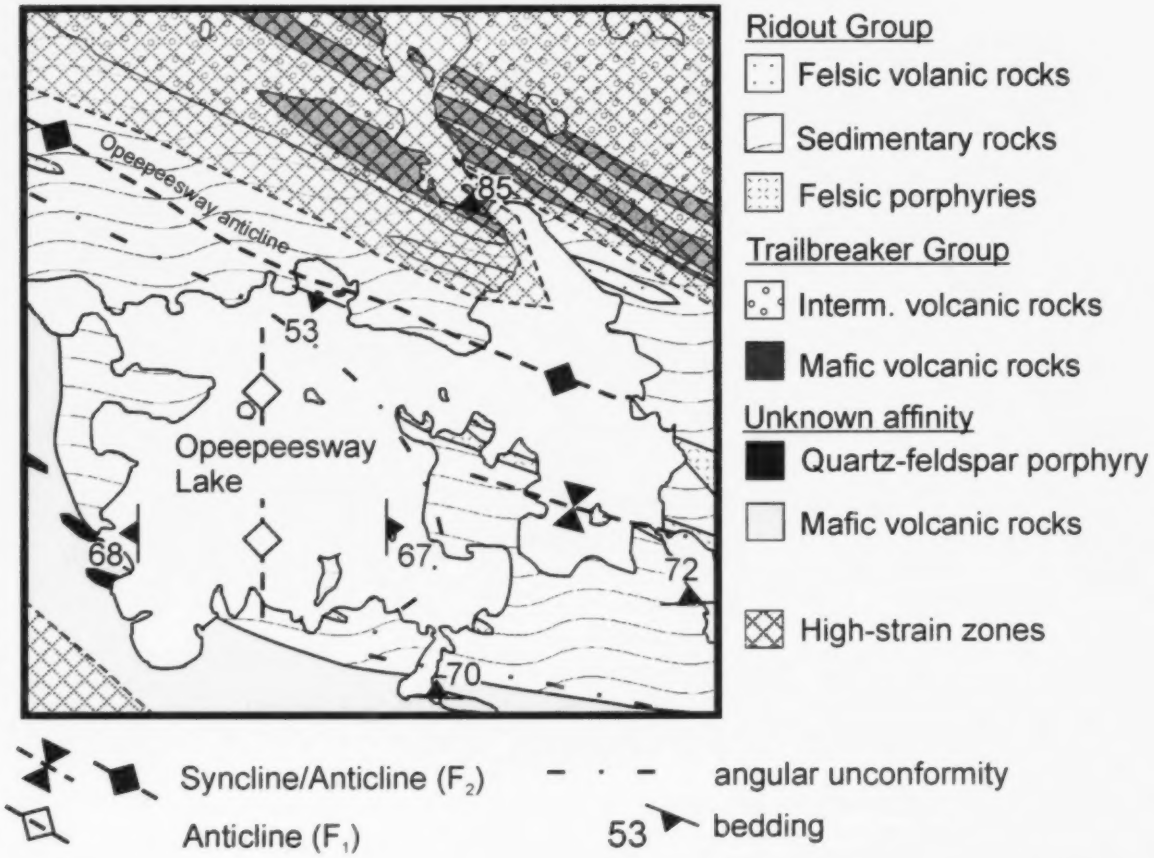

Figure 6. Orientation of bedding planes in the Opeepeesway area of the Swayze greenstone belt. See text for further explanation.

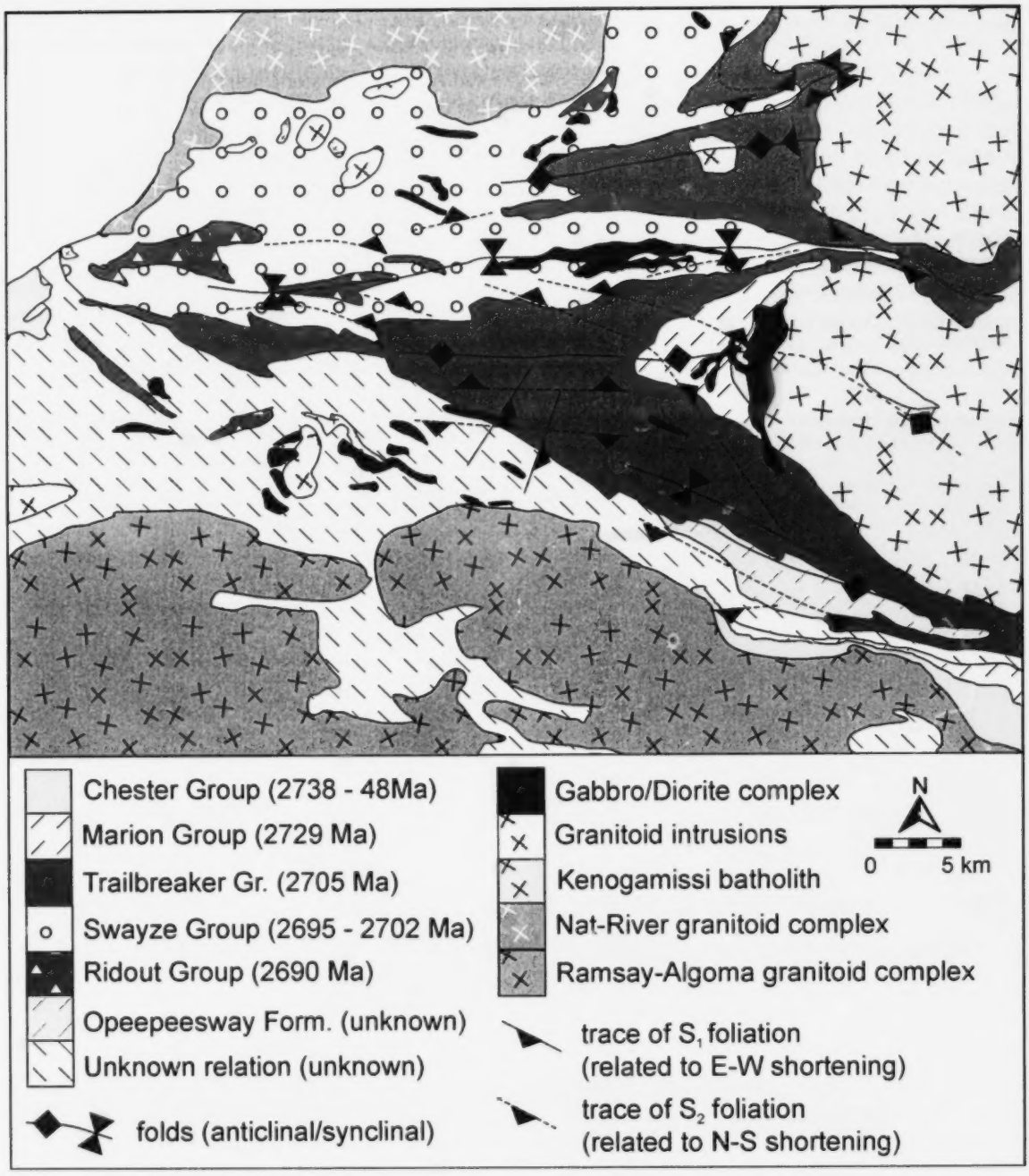

Figure 7. Map of the macroscopic foliation traces in the Swayze greenstone belt. Most of the foliation planes are axial planar to the dominating east-west trending folds. However, some north-south trending foliation planes have been measured that clearly demonstrate the existence of north-south trending folds in the study area.

FOLIATION IN THE SWAYZE GREENSTONE BELT

The macroscopic foliation in the central and western part of the Swayze greenstone belt is axial planar to the dominant east-west trending folds (Figure 7). However, some rare north-south striking foliations are measured. The Schmidt-net projection of the macroscopic foliation planes shows a strong point maxima in the north-northeast indicating steeply dipping foliation planes (Figure 8).

ORIENTATION OF BEDDING IN THE SWAYZE GREENSTONE BELT

Some bedding planes, especially in the Opeepeesway formation (in greywackes underlying the Opeepeesway conglomerates, *see* Figure 6) in the south part of the study area, are oriented north-south facing east or west with generally moderate to steep dips (Figure 9). The steep dips indicate that these bedding planes are not measured in the hinge zone of east-west trending D_2 folds (in which case they would show shallow dips), but that the beds were folded prior to the refolding and, hence, represent north-south oriented D_1 folds. Furthermore, some of the roughly east-west trending bedding planes are overturned. These overturned beds occur close to the margin of the Rice Lake batholith as well as in the centre of the Swayze greenstone belt. The beds close to the batholith margin generally show a margin-parallel trend and, therefore, are interpreted to record the outward push of the batholith during emplacement when they were overturned. In the centre of the Swayze greenstone belt, however, the emplacement of the Rice Lake batholith had no effect on the orientation of bedding planes. The overturned beds here must originate from cross-folding of the sediments and/or volcanic rocks.

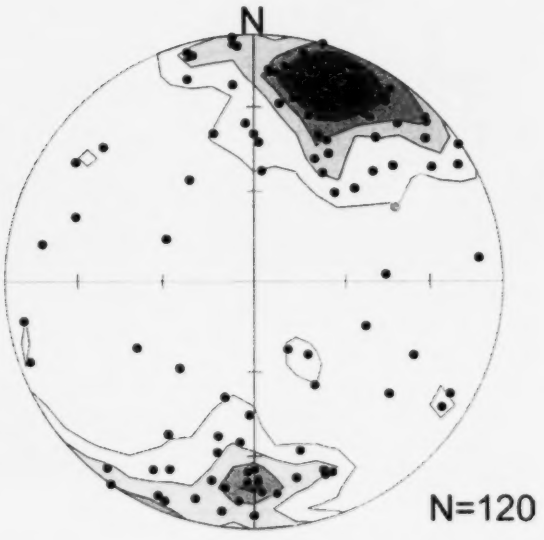

Figure 8. Schmidt net projections of the macroscopic foliation in the Swayze greenstone belt. Only the dominating east-west trending foliation planes are evident.

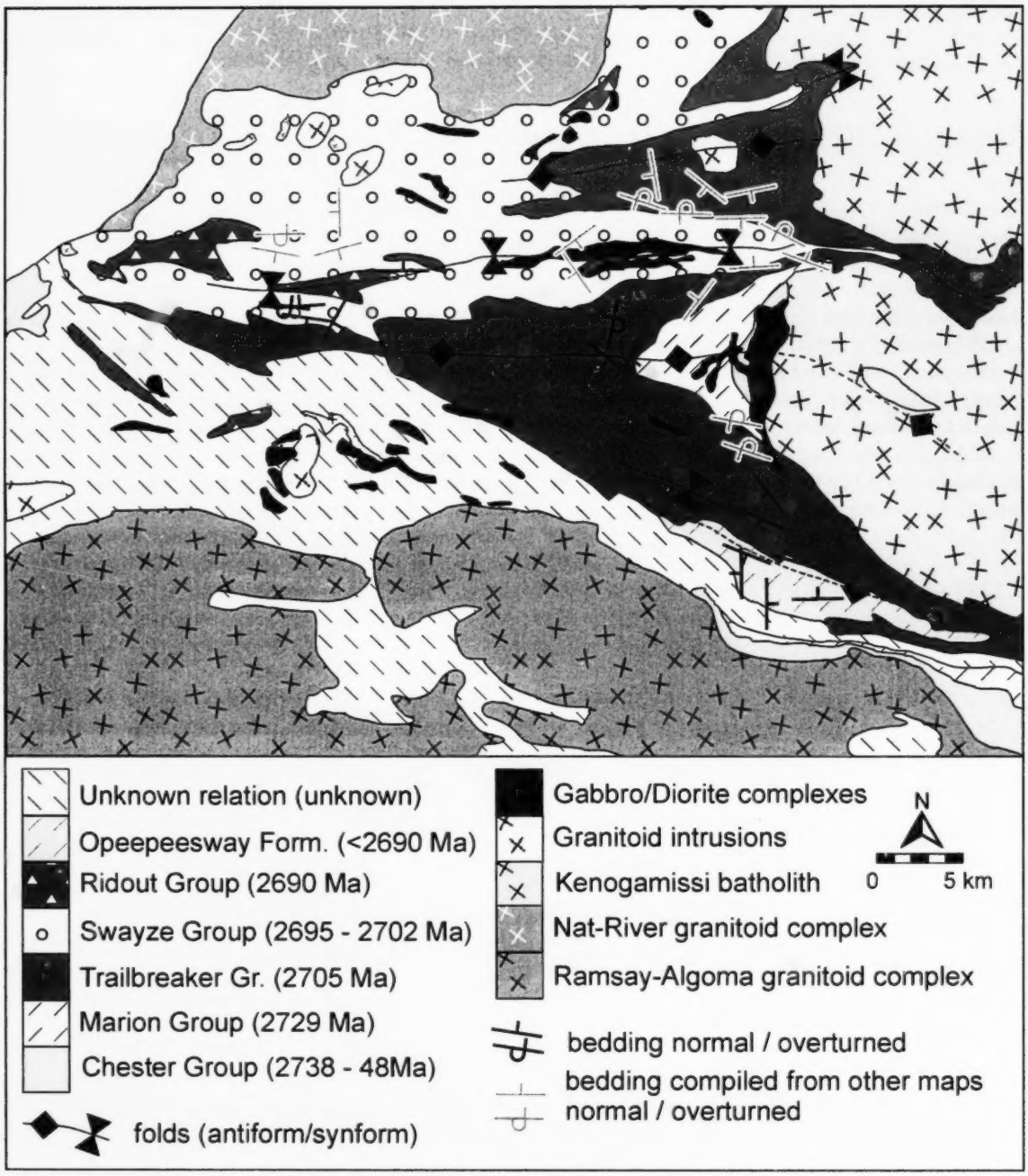

Figure 9. Orientation of bedding in the Swayze greenstone belt. See text for further explanation.

DEFORMATION

Two major tectonic events have been recognized in the field. An earlier deformation event generated north-south trending folds that have been documented in outcrops and at map scale from structural analyses, including younging directions determined using primary structures in sedimentary rocks. Examples of north-south trending F_1 folds documented in the field are shown in Figure 10 in outcrops of the banded iron formation that cap the Woman River formation (Marion group) and in greywackes of the Swayze group, in the centre of the Swayze greenstone belt. Additional evidence for early, north-south trending folds comes from overturned beds (*see* Figures 6 and 9). The second deformation event generated east-west trending folds that now dominate the outcrop pattern throughout the Swayze greenstone belt (*see* Figure 2), and resulted in doubly plunging folds.

No large fault zones have been mapped in the Swayze greenstone belt, however, high-strain zones have been mapped by Heather et al. (1996). While most of these high-strain zones are only of local significance, some (e.g., the Ridout high-strain zone south of the Rice Lake batholith) have been reported to extend into the Abitibi greenstone belt (Milne 1972; Hall 2001; Heather et al. 1995). Milne (1972) suggests that an east-striking shear zone to the north of the Kenogamissi batholith corresponds to the Porcupine–Destor deformation zone in the Abitibi belt. During an investigation of the supracrustal rocks in Denton Township, Hall (2001) was able to verify the existence of the Porcupine–Destor deformation zone north of the Kenogamissi batholith. J.R. Parker (OGS, personal communication, 2002) suggests that the Ridout high-strain zone is the western extension of the Larder–Cadillac deformation zone.

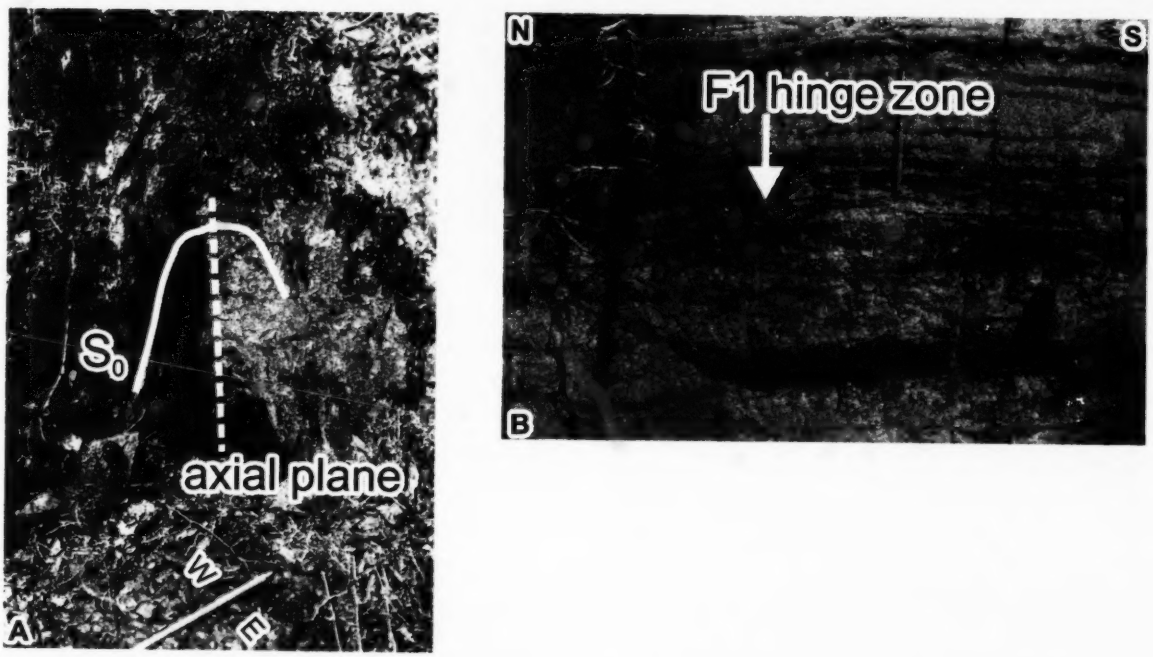

Figure 10. Macroscopic evidence for north-south trending folds. A) North-south trending folds in the iron formations that cap the Woman River formation of the Marion group. B) North-south trending fold in greywackes of the Trailbreaker group. Note that the pencil does not point north, but is only used for scale.

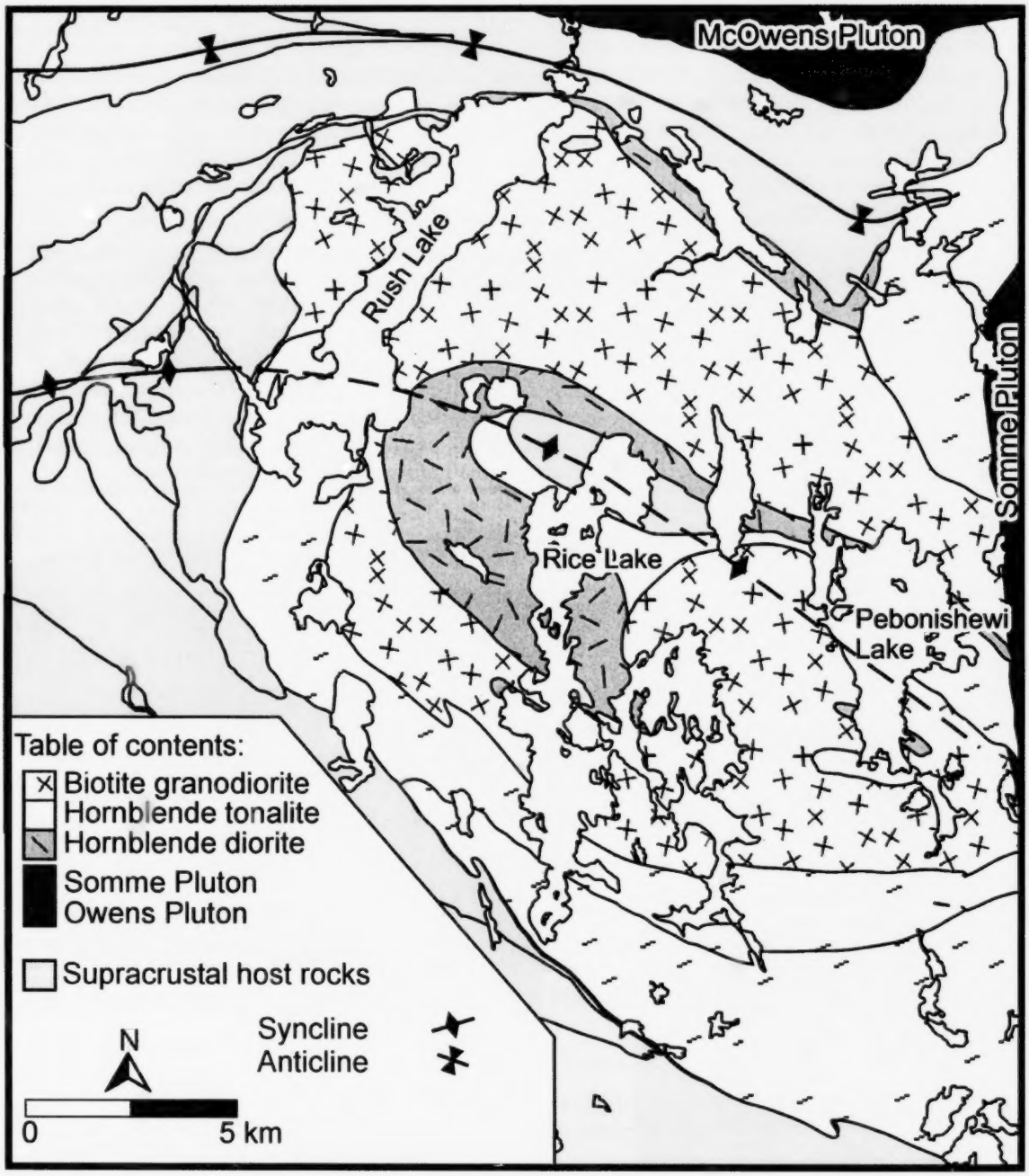

Figure 11. General geology of the Rice Lake batholith (southwestern lobe of the Kenogamissi batholith). See text for further explanation.

Rice Lake Batholith

INTRODUCTION

The Kenogamissi batholith is situated between the Swayze greenstone belt in the west and the Abitibi greenstone belt in the east (*see* Figure 1). Only the western part has extensively been mapped (Heather and Shore 1999; this study); the eastern part is largely unmapped. Geochronological data indicate that the southwestern and possibly the northwestern lobes of the Kenogamissi batholith are older and are essentially synchronous with the age of volcanism, the rest appears to postdate volcanism. Therefore, we refer to the southwestern lobe of the Kenogamissi batholith as the Rice Lake batholith (according to the largest lake in the area) and to the younger part as the Kenogamissi batholith. This study concentrates on the Rice Lake batholith, which abuts on the supracrustal rocks of the Swayze greenstone belt in the north, west and south. In the east, it is truncated by the younger intrusions of the Kenogamissi batholith (e.g., the Somme pluton, Figure 11).

GRANITOID ROCKS OF THE RICE LAKE BATHOLITH

The granitoid rocks of the Rice Lake batholith have been divided into three main groups: hornblende tonalite, biotite granodiorite and hornblende diorite (Heather and Shore 1999; *see* Figure 11).

The hornblende diorite crops out in the centre of the Rice Lake batholith and as a small band along the northern margin (*see* Figure 11). In the centre of the batholith, the hornblende diorite macroscopically appears to be isotropic, while the band at the northern margin shows strong gneissic textures. Therefore, we suggest that these two occurrences of hornblende diorite represent different intrusive events that have intruded at different stages during the two major deformations. In general, the hornblende diorite consists of weakly to strongly foliated, medium- to coarse-grained hornblende diorite to quartz monzonite.

The biotite granodiorite is the largest unit of the Rice Lake batholith (*see* Figure 11). It is a weakly to strongly foliated, fine- to coarse-grained granodiorite with common xenoliths of hornblende tonalite. In some areas, especially in the centre of the Rice Lake batholith, leucocratic granites are common and make up most of the biotite granodiorite.

The hornblende tonalite occurs in the centre of the Rice Lake batholith and as a band at the southern and western margin of the batholith (*see* Figure 11). It is in contact with the surrounding supracrustal host rocks and the granitoids of the younger, posttectonic Somme pluton to the east, which has an age of 2665±2 Ma (Heather and Shore 1999). The tonalite has weak to strong foliations with xenoliths of hornblende diorite to monzodiorite; xenoliths of biotite granodiorite were not observed.

AGE RELATIONSHIP

The age relationship of the three main intrusive events based on crosscutting relationships and xenolith abundance within the different units suggests the following intrusion sequence: hornblende tonalite, biotite granodiorite and hornblende diorite.

From geochronological analyses, ages of 2742±2 Ma for the hornblende tonalite, 2700±1 Ma for the biotite granodiorite and of 2684±1 Ma for the hornblende diorite were obtained (J.W.F. Ketchum, Royal Ontario Museum, written communication, 2002; J.W.F. Ketchum and D.W. Davis, Royal Ontario Museum, written communication, 2001). In the central part of the Rice Lake batholith, an early phase of hornblende diorite exits that is intruded by the biotite granodiorite (Figure 12).

GEOCHEMISTRY

The geochemical analyses of the samples from the Rice Lake batholith were used to further classify the three main units. The total alkali versus silica diagram (TAS; Figure 13a) generally shows a weak cluster of the samples in the quartz diorite and granodiorite field. Although the samples are somewhat altered in sodium, they can be characterized as I-type granites. In the AFM diagram (according to Barker and Arth 1976), the samples all plot in the calc-alkalic field following a trondhjemitic trend (Figure 13b).

The immobile trace-element content of the different rock types can be plotted on discriminant diagrams constructed from the geochemistry of modern plutonic suites with known tectonic activity (Pearce et al. 1984). From these, it is possible to determine the geodynamic setting. However, such

Figure 12. Crosscutting relationships and xenoliths in the Rice Lake batholith. The biotite granodiorite intrudes an early phase of hornblende diorite. Rectangular xenoliths of this early hornblende diorite in the biotite granodiorite are common.

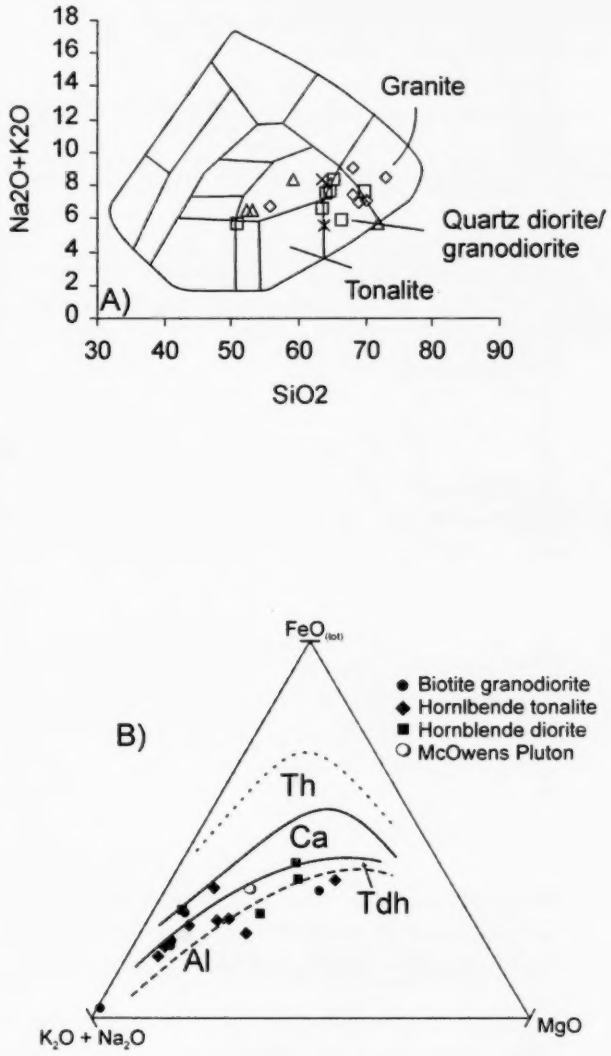

Figure 13. A) Total alkali versus silica diagram. B) AFM diagram according to according to Barker and Arth (1976). See text for further explanation.

diagrams are known to yield ambiguous results if the samples plot close to boundaries between the different tectonic settings (e.g., Foerster et al. 1997). On the Y versus Nb diagram, all the samples plot in the field of volcanic-arc granites and collisional granites (Figure 14a). This can be further differentiated using the (Y+Nb) versus Rb diagram where all the samples unambiguously plot in the field of volcanic-arc granites (Figure 14b) and away from the field boundaries. Furthermore, according to Feng and Kerrich (1992), synvolcanic, syntectonic and late tectonic granitoids are distinguishable according to their variations in $CaO/(Na_2O+K_2O)$ versus SiO_2. Figure 14c demonstrates that most of the analyzed samples show a ratio of major elements typical for syntectonic granites. This clearly demonstrates that the Neoarchean, calc-alkalic granitoids of the Rice Lake batholith have a similar geochemical affinity to Phanerozoic granitic rocks that originated during volcanic-arc formation and deformation and not from collisional events (e.g., terrane accretion).

MACROSCOPIC FOLIATION OF THE RICE LAKE BATHOLITH

The most prominent fabric in the different units of the Rice Lake batholith is the foliation, which, in the field, is defined by the alignment of silicate minerals, biotite ± hornblende. In Figure 15, the trace of the macroscopic foliation is presented. In the hornblende tonalite, especially at the margins of the batholith, a very pronounced foliation can be observed. The leucocratic biotite granodiorite in the centre of the Rice Lake batholith only shows weakly defined foliation planes. However, towards the margins of the biotite granodiorite, the foliation becomes more distinct due to the presence of more abundant biotite crystals.

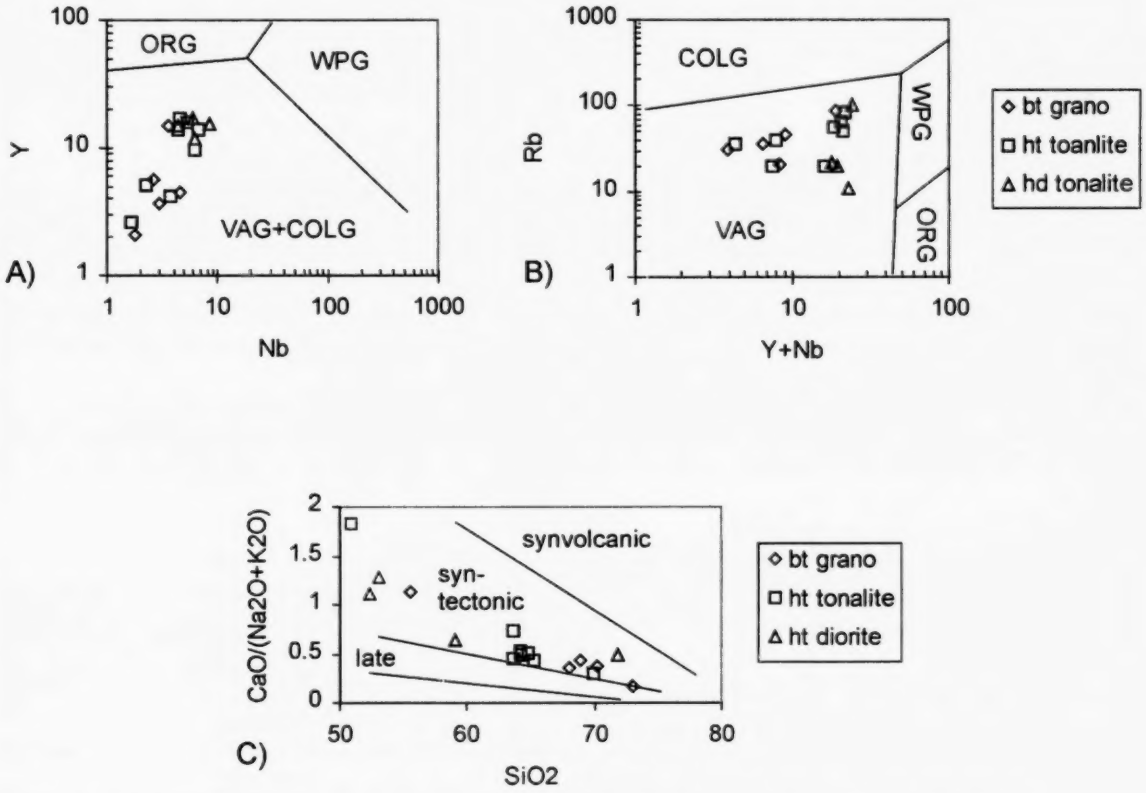

Figure 14. A) Y versus Nb diagram, B) (Y+Nb) versus Rb diagram, and C) geodynamic setting. See text for further explanation.

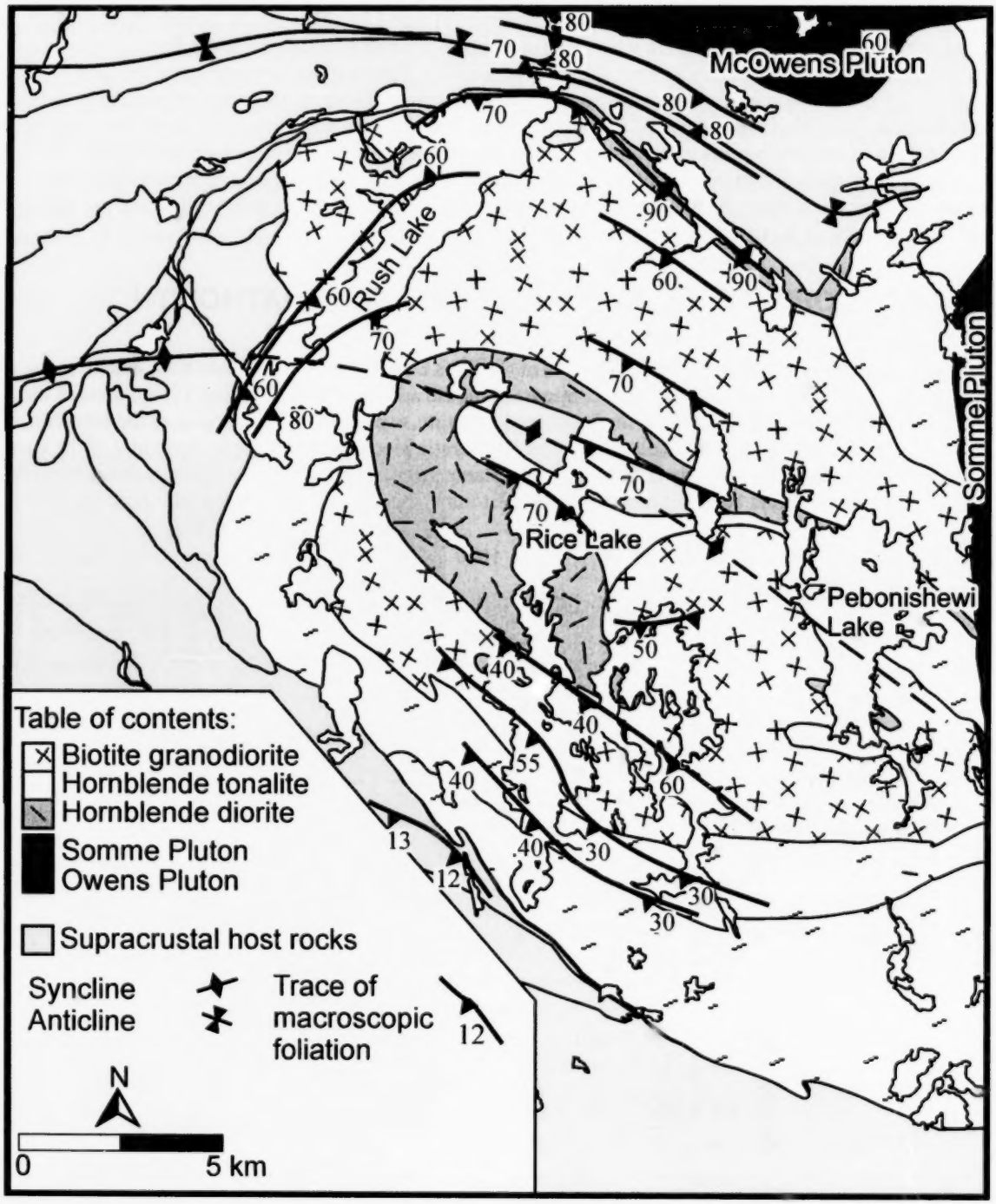

Figure 15. Traces of the macroscopic foliation in the Rice Lake batholith. See text for further explanation.

In the hornblende diorite, a strong foliation grading into gneissic texture was visible at the northern margin. The rocks of the central hornblende diorite macroscopically appear to be isotropic; clear macroscopic foliation planes are sparse and their orientation is ambiguous.

Except for the central hornblende diorite, the other units show very consistent northwest-southeast trends of their macroscopic foliation planes (*see* Figure 15), dipping to the south throughout most of the batholith. Only at the northwestern margin of the batholith, in the biotite granodiorite and the hornblende tonalite, does the foliation tend to be margin parallel with moderate to steep dips. In a north-south profile, dips steepen towards the north where they are nearly vertical. In most of the units, the macroscopic foliation is defined by biotite and/or hornblende. Only in the southern part, close to the batholith margin, do aligned feldspars sometimes define foliation planes.

Crosscutting of the macroscopic foliation is common and can be observed between different granitoid units in the batholith as well as between the granitoid units of the batholith and the surrounding host rocks (*see* Figure 15). Clearly, the macroscopic foliation does not record an emplacement-related orientation of the fabric, but rather documents a regional deformation event during and after emplacement of the different units of the batholith.

PETROGRAPHY

Perpendicular thin sections of selected samples (locations indicated on Figure 16) were prepared to identify microscopic structures and the minerals forming these structures. The samples from the northern and southern parts of the batholith are from areas with very pronounced macroscopic deformation (Figures 18a and 18b).

Thin sections from the northern margin of the Rice Lake batholith (Figure 17) reveal a strong alignment of feldspars and elongated quartz grains in the planes perpendicular to the foliation plane. However, there is no apparent preferred orientation of grains in the foliation plane, giving the rock the appearance of an S-tectonite.

This fabric can also be observed in the northern marginal areas of the biotite granodiorite. In the central part of the batholith, which mainly is occupied by the biotite granodiorite, magmatic to submagmatic fabrics are preserved (Figure 18c).

In the southern part of the Rice Lake batholith (in the hornblende tonalite, *see* Figure 16), feldspars and elongated quartz grains are aligned in the foliation plane as well as in the planes parallel and perpendicular to the lineation (S-tectonite, Figure 19). These fabrics suggest flexural shear on the limb of a fold.

Furthermore, the hornblende tonalite and hornblende diorite (Figure 18d) show a strong metamorphic overprint of their fabric.

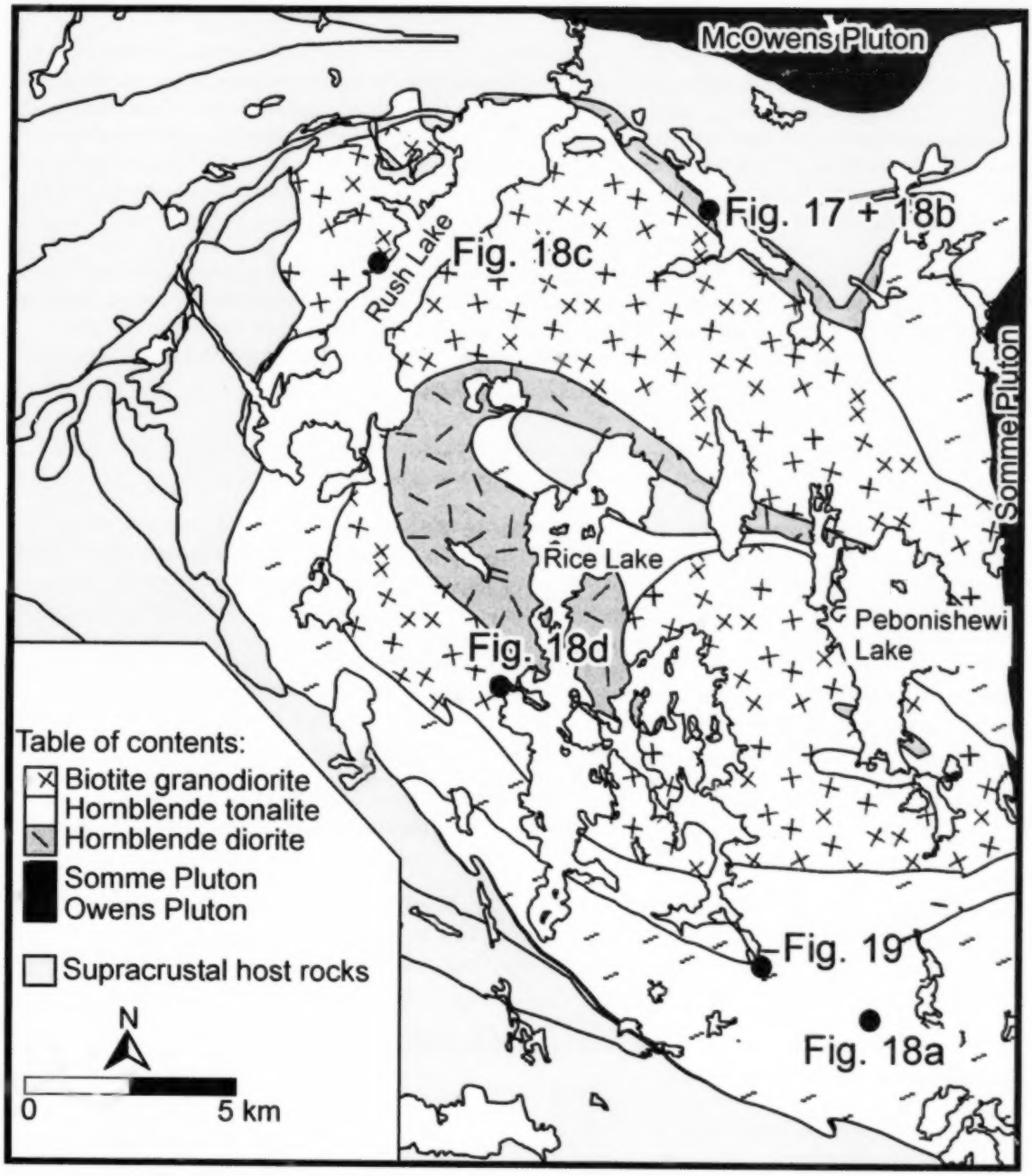

Figure 16. Location map of thin sections and outcrops shown in Figures 17, 18 and 19 and described in the text. Thin sections from the northern margin were cut from samples of the gneissic hornblende diorite, whereas samples at the southern margin were taken from gneissic tonalite.

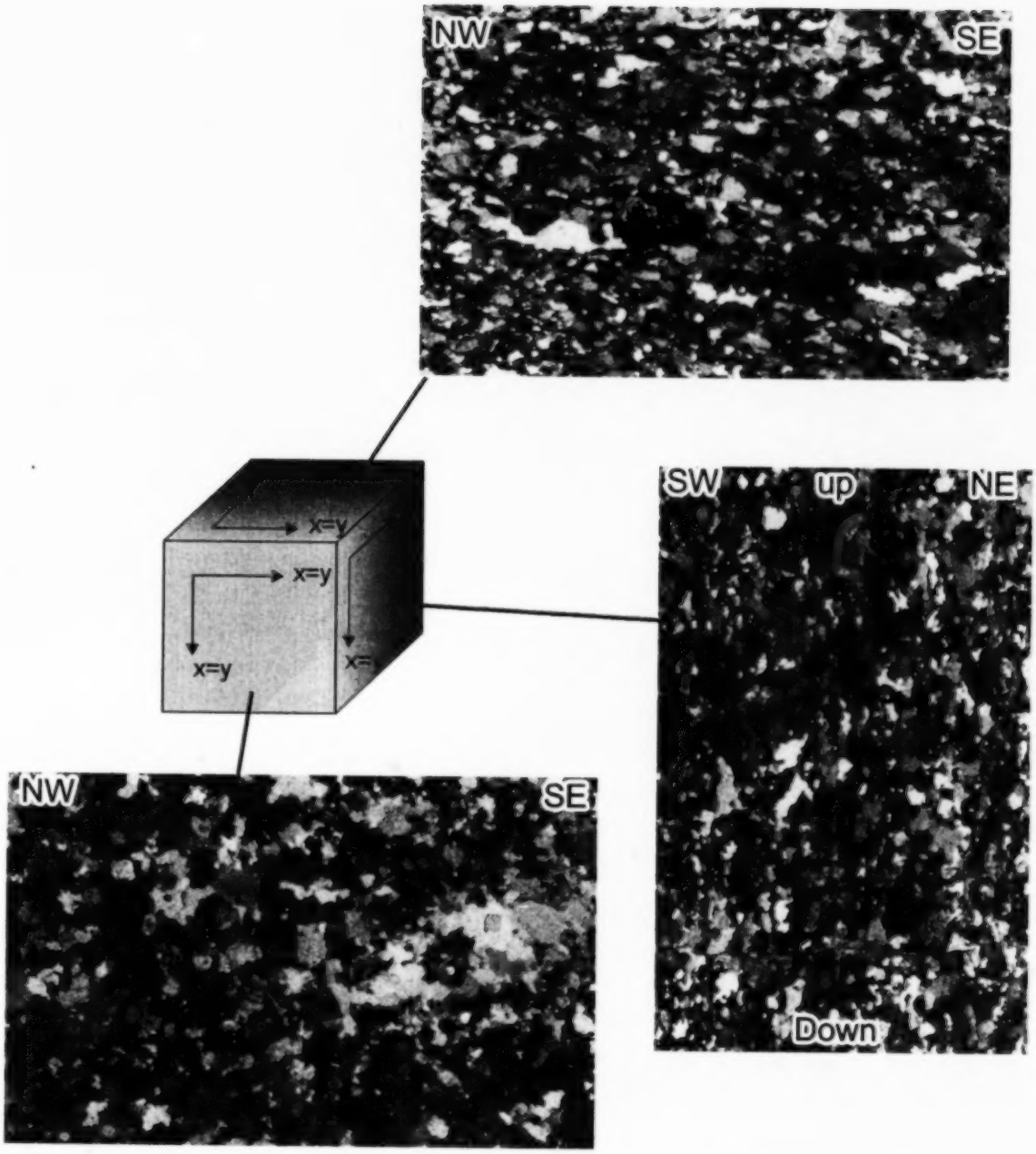

Figure 17. Thin sections of hornblende diorite from the northern margin (JB199, *see* Figure 16 for location). A) parallel to the foliation, B) parallel to the lineation/perpendicular to the foliation and C) perpendicular to the foliation and lineation.

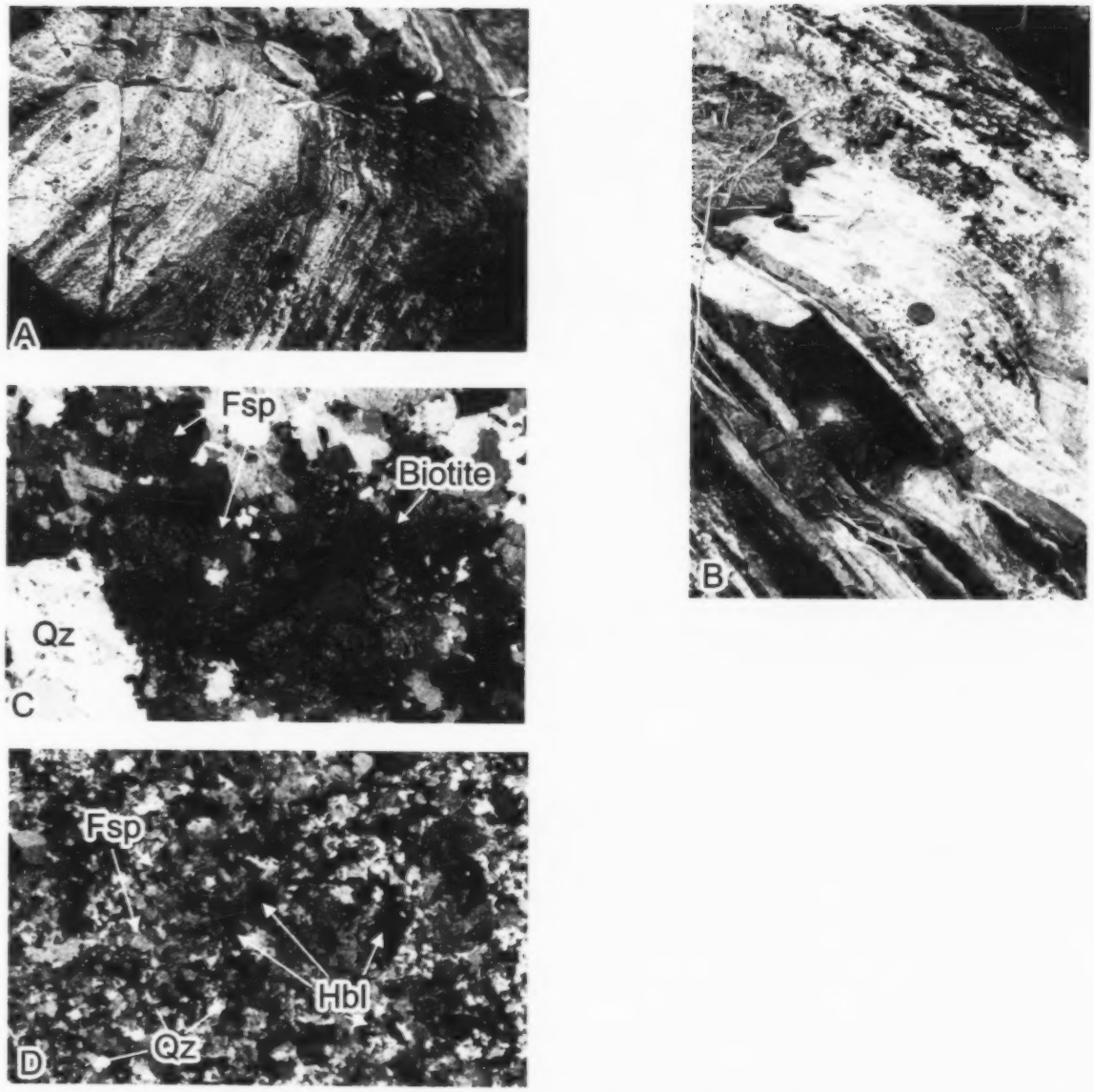

Figure 18. All sample locations are shown in Figure 16. A) Granitoid rocks with gneissic texture from within the Ridout high-strain zone at the southern margin of Rice Lake batholith. B) Granitoid rocks of the hornblende diorite at the northern margin of Rice Lake batholith. C) Thin section of the biotite granodiorite. No strong submagmatic or solid-state deformations can be observed. D) Thin section of a hornblende diorite sample with a strong metamorphic overprint from near the centre of Rice Lake batholith.

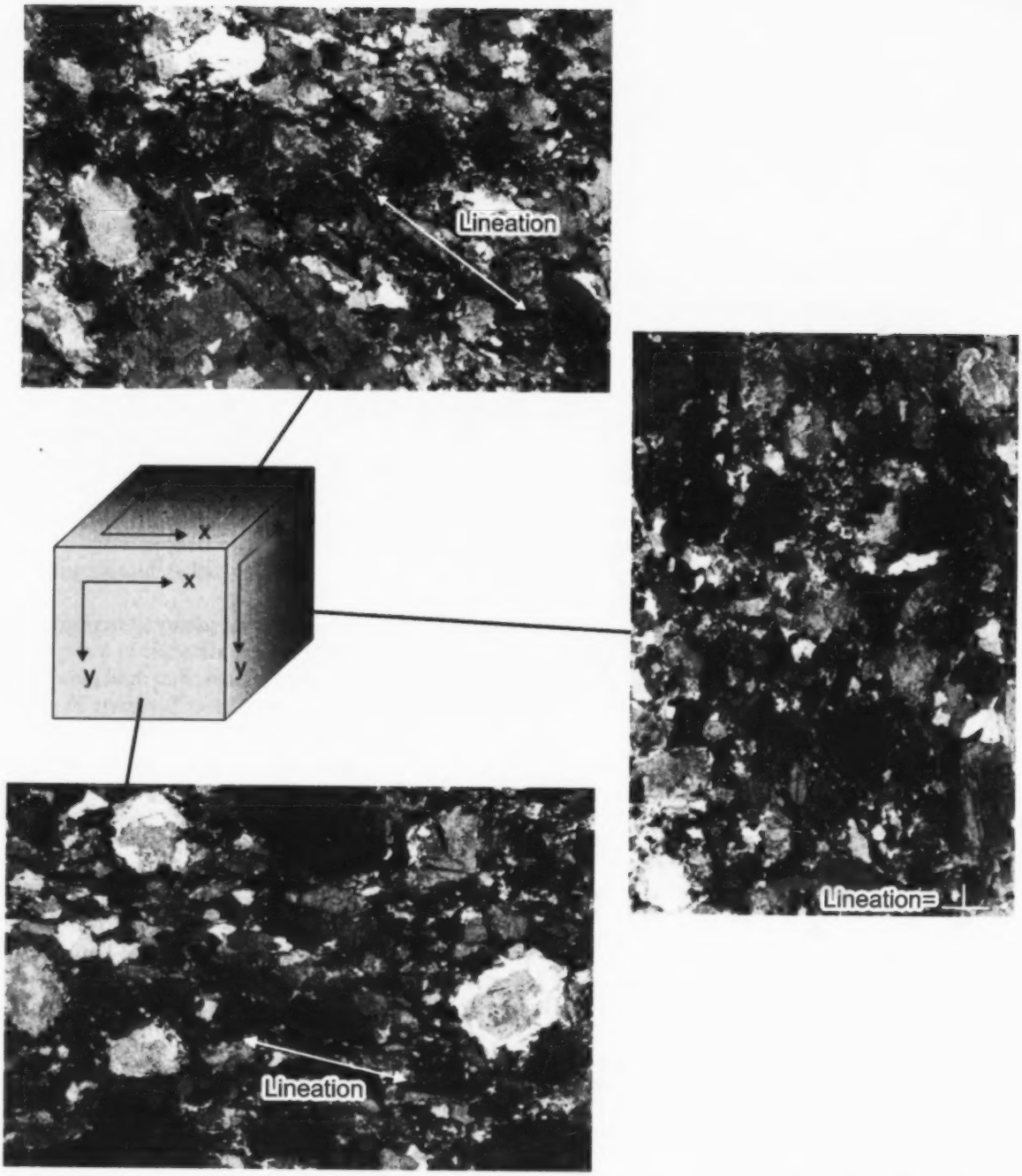

Figure 19. Thin sections of hornblende tonalite from the southern margin (JB100, *see* Figure 16 for location). A) parallel to the foliation, B) parallel to the lineation/perpendicular to the foliation and C) perpendicular to the foliation and lineation.

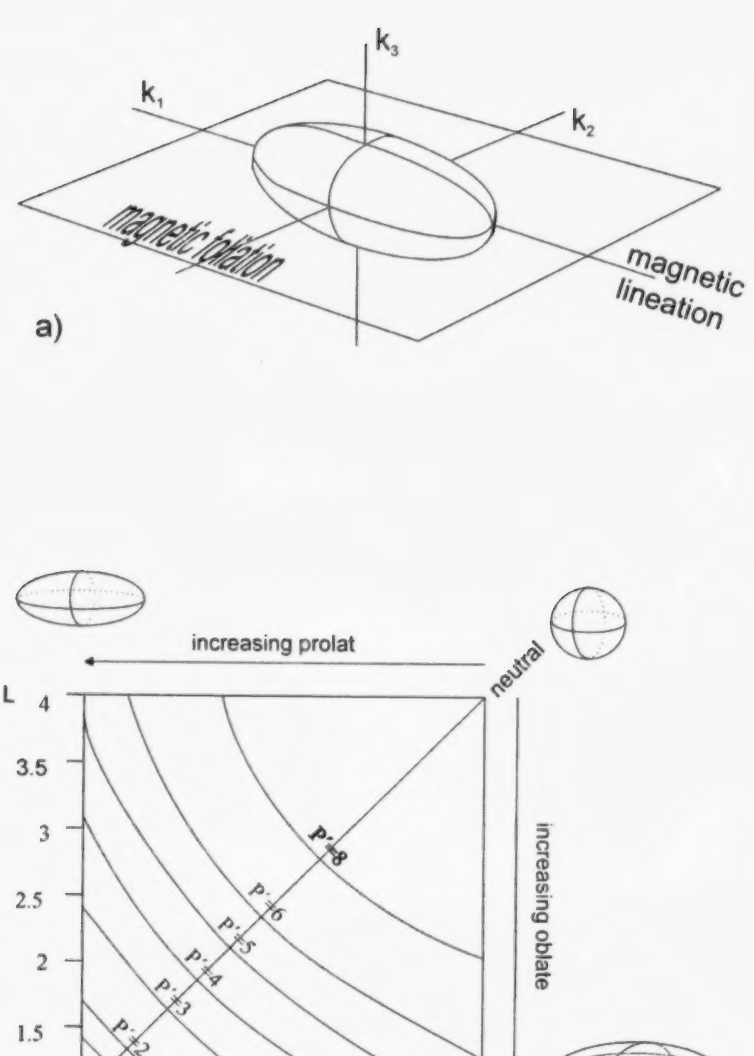

Figure 20. A) Representation of the three main magnetic axes and their bulk values through the so-called magnetic ellipsoid. The longest (K_1) and intermediate (K_2) axes represent the magnetic foliation; K_1 is also the magnetic lineation. K_3, the shortest axis, is perpendicular to the magnetic foliation and, thus, can be used as the pole point to the magnetic foliation plane in schmidt net projections. B) Since all of the calculated parameters used in this study depend on the ratio of the value of the different main magnetic axes, they show a mathematical dependence (*modified from* Jelinek (1981) and *from* Borradaile and Craig (1987)).

MAGNETIC MEASUREMENTS OF GRANITOID ROCKS

Introduction

In this study, the anisotropy of the magnetic susceptibility (AMS) was measured to enhance the field observations and structural measurements. With this measurement method, it is possible to detect even very weak (magnetic) fabrics in rocks that macroscopically appear to be isotropic.

The magnetic properties of a rock are caused by the magnetic properties of the minerals in the rock. Principally, three different types of magnetic behaviour exist, each mineral belongs to one of these types (Tarling and Hrouda 1993).

Diamagnetic minerals:
Diamagnetic minerals have very weak magnetic properties and, in the case of granitoid rocks, only marginally affect the magnetic measurements. Their bulk susceptibility is, by definition, negative and very low (Tarling and Hrouda 1993). Some of the most common minerals have diamagnetic properties (quartz, feldspar, etc.).

Paramagnetic minerals:
Paramagnetic minerals are the most important minerals in the study of the AMS of granitoid rocks. Their bulk susceptibility (by definition positive) depends to some extend on the iron content of the minerals (Tarling and Hrouda 1993). Biotite and hornblende are, in this study, the most important minerals with paramagnetic properties, since their orientation records the deformation and emplacement related fabric of the granitoid rocks.

Ferrimagnetic minerals (*sensu lato*):
This group of minerals can most strongly influence the magnetic properties of a rock sample, since they have very high bulk susceptibilities (by definition positive, Tarling and Hrouda 1993). In case of an AMS study of granitoid rocks, magnetite usually is the most common ferrimagnetic mineral (*sensu lato*). Even if the magnetite content of the sample is low, the magnetic properties of magnetite can still dominate the magnetic properties of the sample. Furthermore, magnetite has a shape anisotropy, meaning that the orientation of the three main magnetic axes depends on the shape of the grain rather than its crystallographic (cubic) shape (opposed to, for example, biotite or hornblende where the orientation of the crystallographic axes defines the orientation of the main magnetic axes in any given grain).

Magnetic Properties

During the AMS measurements, different parameters are measured that all result from the ratio and orientation of the three main magnetic axes and their susceptibilities (Figures 20a and b). In this study, the bulk susceptibility, the shape of the magnetic ellipsoid (T), the corrected degree of anisotropy (P′) and the orientation of the magnetic foliation and lineation are used. Anisotropy of magnetic susceptibility (AMS) data are included in Appendix 1.

The bulk susceptibility of a sample can be used to estimate what kind of minerals dominate the magnetic properties of the rocks (diamagnetic, paramagnetic or ferrimagnetic). The shape of the magnetic ellipsoid and the corrected degree of anisotropy show how distinct the magnetic foliation and lineation is. In addition, P′ can, to some extent, also be used to determine the dominant group of minerals (diamagnetic, paramagnetic or ferrimagnetic) in the measured sample.

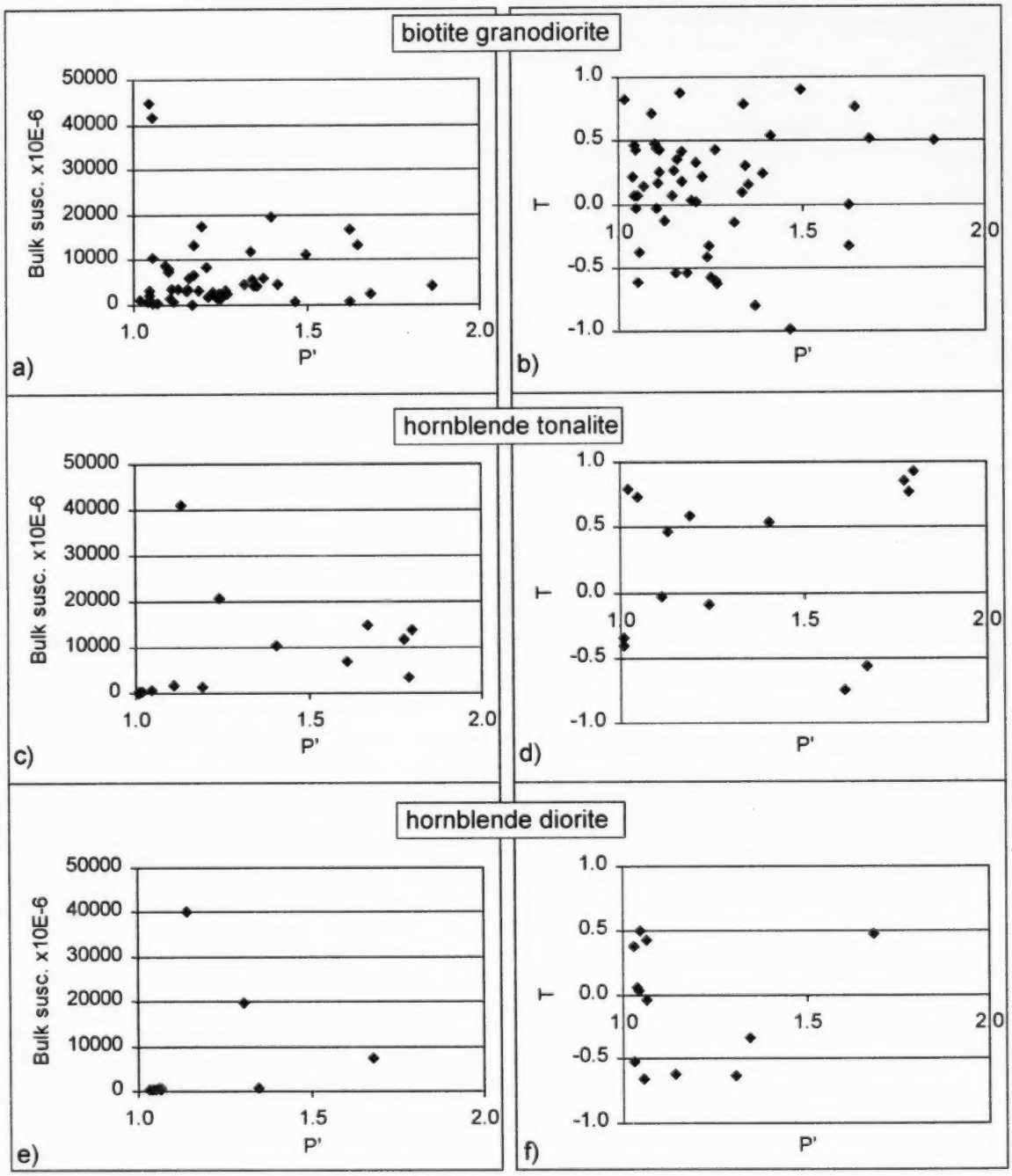

Figure 21. Susceptibility diagrams for the three main units of the Rice Lake batholith. In a), c) and e), the bulk susceptibility is plotted versus the degree of anisotropy. In b), d) and f), the shape of the magnetic ellipsoid is plotted versus the degree of anisotropy. Diagrams a) and b) represent values from the biotite granodiorite, c) and d) from the hornblende tonalite, and e) and f) from the hornblende diorite. For further explanation, see text.

As can be seen in Figures 21a, 21c and 21e, the bulk susceptibilities of all three units suggests, at least for some samples, a varying influence of ferrimagnetic minerals on the bulk susceptibility and, therefore, on the orientation of the magnetic foliation and lineation. The bulk susceptibility of the biotite granodiorite is low; only a few outliers with bulk susceptibilities up to 45 000$\times 10^{-6}$ SI exist, and most of the samples show bulk susceptibilities below 10 000$\times 10^{-6}$ SI (*see* Figure 21a). This indicates that the magnetic properties of some of the samples are dominated by ferrimagnetic minerals (*sensu lato*). However, thin section analyses revealed that magnetite replaces biotite and hornblende. Due to the shape anisotropy of magnetite, its main magnetic axes are oriented subparallel to the main magnetic axes of the grain it replaces. Therefore, the orientation of the magnetic foliation and lineation still reflects the orientation of the original magnetic foliation/lineation of the samples that was recorded during emplacement and/or deformation. The shape of the magnetic ellipsoid of the biotite granodiorite mainly is oblate, only some samples reflect a pronounced prolate shape of the magnetic ellipsoid (Figure 21b).

The hornblende tonalite shows two groups of samples (*see* Figure 21c). One set of samples has high bulk susceptibilities and/or high degrees of anisotropy, while the other set shows very low bulk susceptibilities (in the range of 600$\times 10^{-6}$ SI) and a low degree of anisotropy (ranging from 1.0 to 1.3, *see* Figure 21c). While the set of samples with high degrees of anisotropy and high bulk susceptibilities clearly is dominated by ferrimagnetic minerals, the other set clearly reflects the orientation of biotite and/or hornblende. The shape of the magnetic ellipsoid of the different samples ranges between highly oblate to moderately prolate with no apparent systematic order concerning the two sets (Figure 21d).

The hornblende diorite is comparable to the hornblende tonalite. Two sets of samples exist, one that is clearly dominated by ferrimagnetic minerals, whereas the other set only shows a very low content of ferrimagnetic minerals (*see* Figure 21e). Again, the shape of the magnetic ellipsoid of the different samples shows no systematic order and ranges between oblate and prolate (Figure 21f).

Magnetic Foliation

In Figure 22, traces of the magnetic foliation in the Rice Lake batholith are shown. They show great similarities in both, orientation and dip, with the macroscopic foliation (*see* Figure 15). The magnetic foliation shows a consistent southeast-northwest trend dipping to the southwest, except for within the central hornblende diorite, and at the northwestern margin of the batholith, where the magnetic foliation appears to be margin parallel. In addition, the foliation frequently crosscuts internal boundaries of the different granitoid units as well as external boundaries to the surrounding host rocks. The majority of magnetic foliations in the southern part of the Rice Lake batholith are moderately dipping, at the northern margin and, where the magnetic foliation is margin parallel, dipping angles are only shallow (Figures 22 and 23). In the central hornblende diorite, the magnetic foliation shows a consistent north-south orientation with shallow to moderate dips to the east and west.

The magnetic foliation frequently crosscuts boundaries between the different granitoid units as well as boundaries to the surrounding host rocks. Similar to the macroscopic foliation, the magnetic foliation does not record an emplacement fabric, but rather records a deformation fabric generated during or after the emplacement of the granitoid rocks. Thin section analyses revealed that the hornblende diorite and hornblende tonalite show solid-state deformation; therefore, the recorded magnetic fabric must have been generated after the intrusion and emplacement of these units.

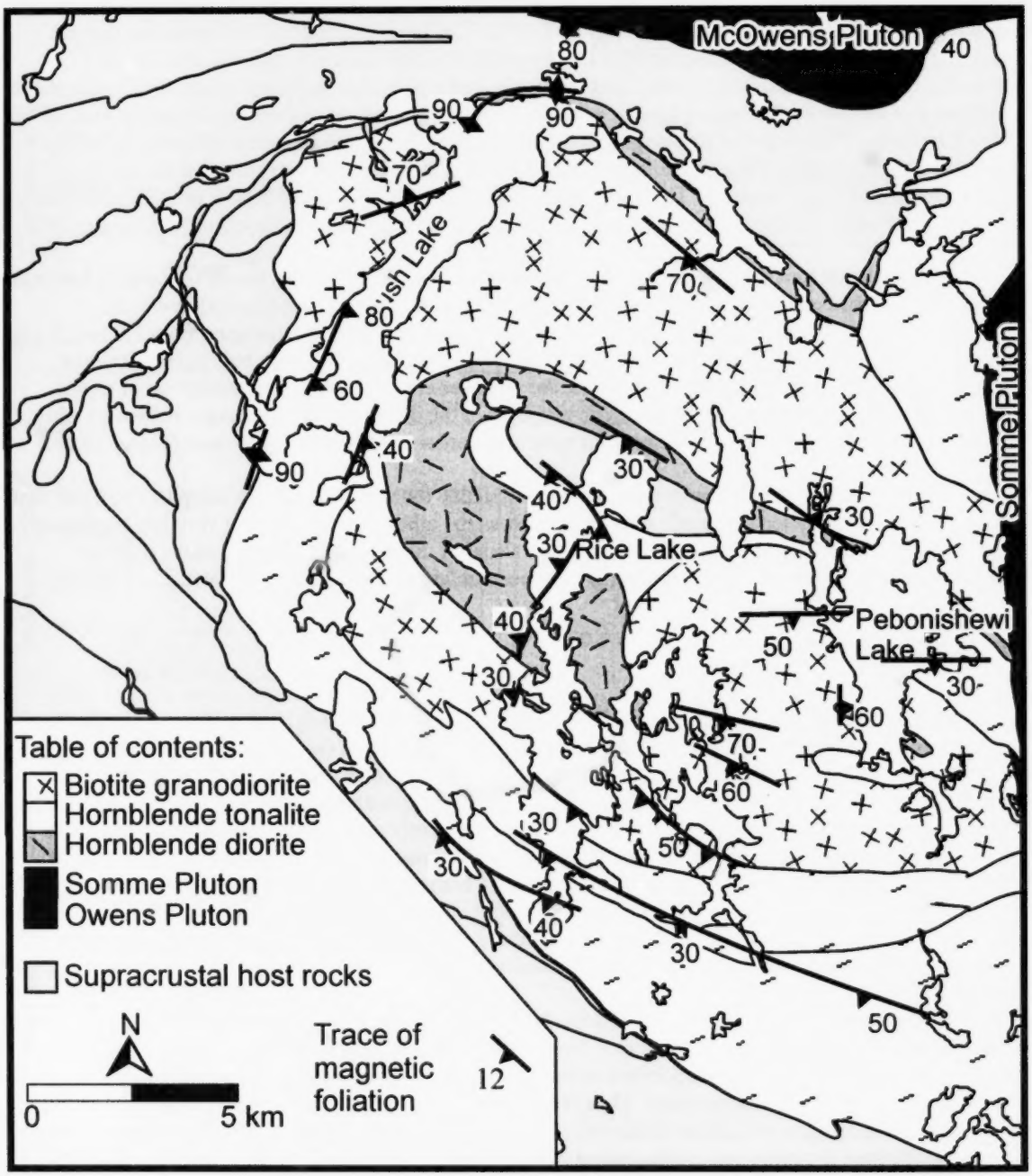

Figure 22. Traces of the magnetic foliation in the three main units of the Rice Lake batholith. See text for further explanation.

Magnetic Lineation

The magnetic lineation displays a less consistent trend than the magnetic foliation (Figure 24). In the northern and northwestern part of the batholith, it appears to be oriented parallel to the outer margin (with variable plunge, Figure 25), whereas, in the central and southern parts of the batholith, it shows a uniform east-west orientation. The plunge of the magnetic lineation changes throughout the batholith. At the southern margin in the gneissic textured hornblende tonalite, the magnetic lineation plunges to the southeast, whereas, in the less deformed units at the southern margin, it plunges to the northwest (*see* Figure 24). We interpret this to reflect the presence of a sinistral shear zone at the southern margin of the batholith.

Towards the central part of the batholith, the magnetic lineation in the east plunges to the east, whereas in the west, it plunges to the west. In both cases, the magnetic lineation roughly parallels the axial surface trace of the Woman River anticline (*see* Figure 15) and, therefore, indicates the fold axis is doubly plunging.

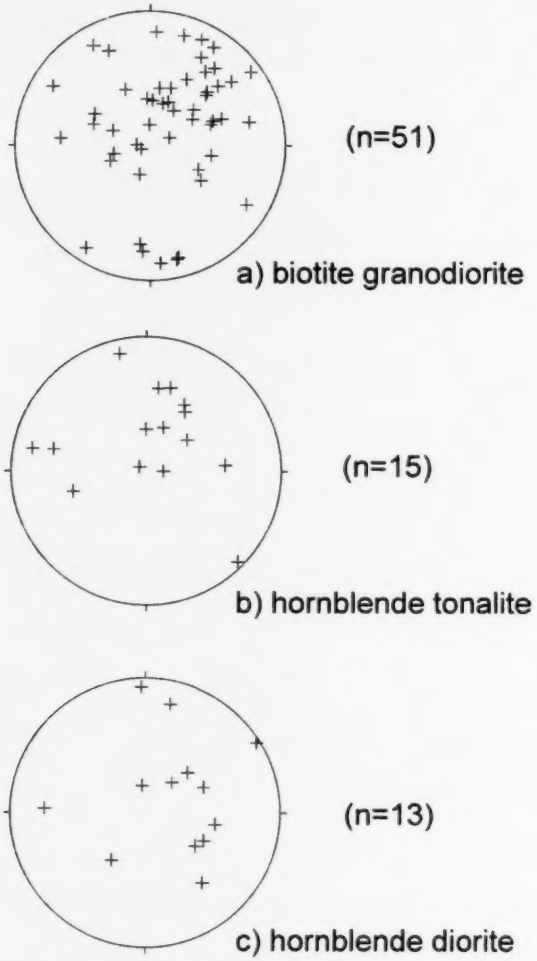

Figure 23. Schmidt net projections of the magnetic foliation (lower hemisphere): a) biotite granodiorite, b) hornblende tonalite and c) hornblende diorite. See text for further explanation.

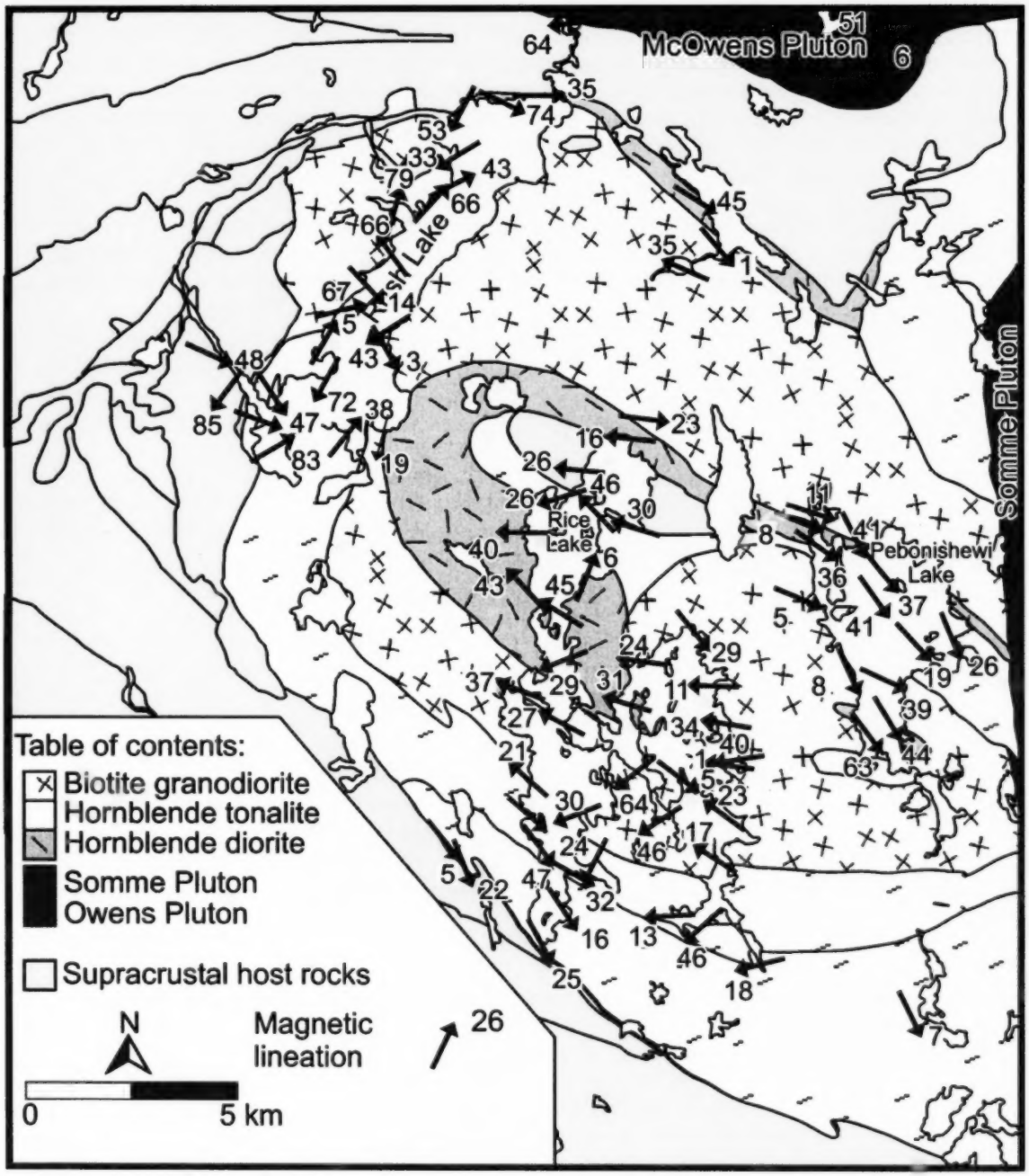

Figure 24. Map of the magnetic lineation. See text for further explanation.

DEFORMATIONS OF THE RICE LAKE BATHOLITH

Two major deformation events affected the different units in the Rice Lake batholith. The first deformation event, a east-west shortening, is only visible in the hornblende diorite and is recorded as a north-west trending magnetic foliation. The second event was a regional east-west folding possibly during north-south compression. The east-west trending Woman River anticline extends from the supracrustal rocks in the Swayze greenstone belt to the west into the batholith (*see* Figure 15). A shear zone with flexural slip may have occurred within the hornblende tonalite at the southern margin of the Rice Lake batholith along the southern limb of the Woman River anticline during this east-west folding event.

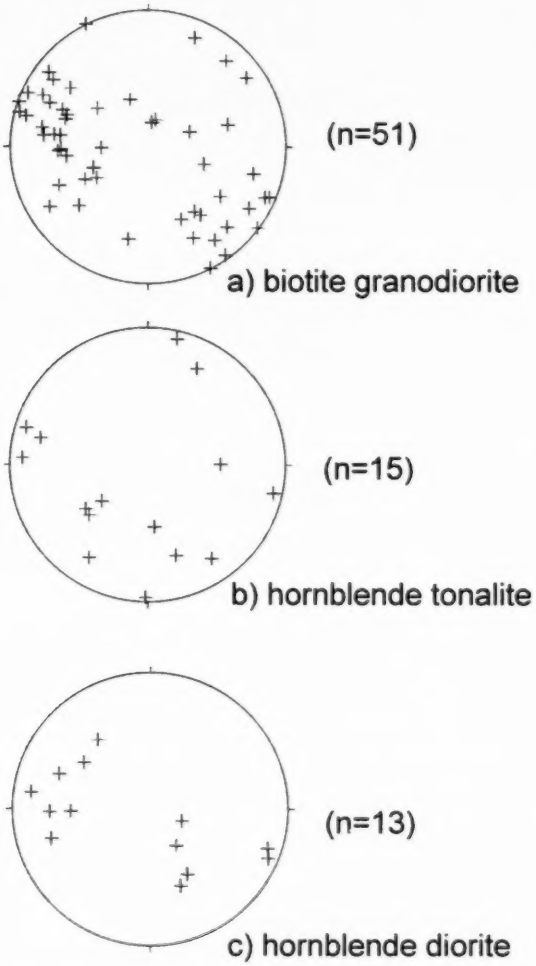

Figure 25. Schmidt net projections of the magnetic lineation (lower hemisphere): a) biotite granodiorite, b) hornblende tonalite and c) hornblende diorite. See text for further explanations.

Summary

SWAYZE AND ABITIBI GREENSTONE BELTS

The structural and reconnaissance mapping of the Swayze greenstone belt has revealed a close relationship to the Abitibi greenstone belt in the east. It has been shown that, with the available geochronological data and stratigraphic interpretations, correlation of the two belts can be made. The Opeepeesway conglomerates, however, should be separated from the Ridout group, as they show very strong similarities to the conglomerates in the Timiskaming assemblage (granitoid cobbles, red cherts, etc.) and also have an unconformable contact with the underlying units of the Ridout group.

Tectonic fabrics in the Swayze greenstone belt provide evidence for two folding events, an earlier set of north-south trending folds and a later set of east-west trending folds. The north-south trending, earlier set of folds was documented in iron formations of the Marion group as well as in greywackes of the Ridout group. No evidence for north-south folding was observed in the Opeepeesway conglomerates unconformably overlying the Ridout group greywackes. This indicates that the north-south deformation must have occurred shortly after the deposition of the greywackes in the Ridout group, but before the deposition of the Opeepeesway conglomerates. According to the available geochronological data, the earlier deformation must have occurred after ca. 2690 million years ago (*see* Table 1). The later deformation affected all the units of the Swayze greenstone belt, including Timiskaming-age volcanic rocks in the core of the Brett Lake syncline, thus providing the maximum age of ca. 2680 Ma for D_2 (Ayer et al. 2002b).

The most significant difference between the two belts is the abundance of komatiites in the Abitibi greenstone belt and their relative lack in the Swayze greenstone belt. Whereas the relatively large volumes of komatiites were deposited in the Abitibi greenstone belt, volcanism in the Swayze greenstone belt mainly produced mafic to felsic volcanics. Thus, it appears that the plume responsible for the komatiite had less impact on the Swayze greenstone belt.

RICE LAKE BATHOLITH

Pre-tectonic granitoid intrusions were observed in the southwestern part of the Kenogamissi batholith. Most of the exposed parts of the batholith are younger posttectonic granitoids. In the Rice Lake batholith, three distinctive units of tonalitic, granodioritic and dioritic composition have been observed. Field observations and geochemical analyzes showed that the different units reflect a wide variety of different granitoid rock types; their allocation to these general rock classifications is thus only a generalization. Field observations of the biotite granodiorite show that this unit is leucocratic in the central part, whereas, close to the margin, it contains coarser grained biotite, hornblende and feldspar. The hornblende tonalite and the hornblende diorite at the margins of the batholith are strongly deformed and typically gneissic. Only in the central part of the batholith does the hornblende diorite appear to be macroscopically isotropic. Therefore, we suggest that the hornblende diorite at the northern margin, which has a pronounced gneissic texture, is a different unit.

The structural investigation in the Rice Lake batholith revealed a pronounced macroscopic foliation with a very uniform northwest-southeast orientation, where it is not margin parallel. If a fabric is solely the result of the emplacement as a granitoid diapir or granitoid balloon, the macroscopic foliation is margin parallel throughout the intrusion. The difference between ballooning and diapirism is the orientation of lineations throughout the intrusion. During the emplacement of a laccolithic body, the

foliation generally follows a stable trend throughout the laccolith. The fabric measured with the various measurement methods in this structural study of the Rice Lake batholith revealed a strongly deformed fabric that is inconsistent with its development by a diapiric or ballooning emplacement of the batholith. Rather the orientation of the macroscopic and the magnetic foliations record regional deformation fabrics developed during or after emplacement of the batholith.

The metamorphic aureole around the margin of the batholith mapped by Heather and Shore (1999) is typically very narrow extending only a few hundred metres into the surrounding host rocks. A similar narrow metamorphic aureole was observed in the Chinamora batholith in Zimbabwe by Becker et al. (2000) and Siegesmund et al. (2002). Thermal modelling of the ascent and emplacement of this Neoarchean granitoid complex showed that the multiple intrusions that form the Chinamora batholith cannot have been very thick (Siegesmund et al. 2002). With its relatively small contact metamorphic aureole, this model should also applies to the Rice Lake batholith.

Thin section analyses revealed fabrics in the different granitoid units recording metamorphism and differing strain orientations. Both the hornblende diorite and hornblende tonalite show a strong metamorphic overprint and common solid-state deformation. In only a few thin sections of the biotite granodiorite was a non-penetrative, solid-state deformation fabric observed. Most of the thin sections of the biotite granodiorite show evidence of magmatic or submagmatic fabric. Only at the northern margin of the biotite granodiorite did the thin section analyses reveal the same kind of solid-state deformation that was observed in the neighboring hornblende diorite. The deformation that led to the formation of the observed high-strain zone at this margin must have ceased prior or during the intrusion of the biotite granodiorite. Bouchez et al. (1992) have shown that the division between the magmatic and submagmatic states for leucogranites occurs at a temperature difference of only 4°C, while for tonalites it occurs in the range of 63°C. During cooling of thin sheets of leucogranites, this temperature difference would have been passed relatively quickly. Therefore, the biotite granodiorite shows solid-state fabrics close to its margins, where it was cooled quickly by the surrounding host rocks, whereas in the centre, where the cooling rate and possibly the strain was much lower, it was insufficient to develop solid-state fabrics.

At the southern margin in the Ridout high-strain one, evidence for solid-state deformations is also common in the hornblende tonalite. Here, the tonalite shows a strong mineral alignment of quartz, feldspars, hornblende and biotite in the foliation plane as well as in planes perpendicular to the foliation plane (parallel and perpendicular to the lineation). Heather et al. (1995) mapped part of the Ridout high-strain zone within an intrusion he called the Neville pluton. Our investigations indicate the Neville pluton is a highly deformed part of the Rice Lake batholith and, hence, is included within the hornblende tonalite unit of the batholith (*see* Figure 15).

The measured fabrics in the Rice Lake batholith do not record the emplacement-related fabrics, but rather record deformation events. The first deformation event (north-south folding) is only recorded in the hornblende diorite in the central part of the batholith. The later east-west folding event affected all other units of the batholith. Cross-folding of the two sets of folds may have enhanced uplift and exhumation of the batholith. During this rapid uplift, erosion of the granitoid rocks may have supplied some of the granitoid cobbles found in the Opeepeesway and Timiskaming conglomerates, which occurred in topological depressions surrounding the batholiths.

Due to the large rheological contrast of the granitoid rocks and the surrounding supracrustal host rocks, shear zones were developed at the northern and southern margins of the batholith. At the southern margin, flexural slip in the granitoids is recorded by the magnetic lineation. The dip of the macroscopic and magnetic foliations at the southern margin ranges between 30 and 40° to the southwest, whereas, in the host rocks, it is in the range of 10 to 20°. This suggest that the Rice Lake batholith extends below the Swayze greenstone belt to the south and that the greenstone belt rocks were thrust onto the batholith (batholith-side down).

At its northern margin, the Rice Lake batholith was pushed against the Kenogamissi batholith. This led to the vertical foliation planes in the Rice Lake batholith and in the infolded supracrustal host rocks that separate the Rice Lake batholith from the Kenogamissi batholith to the north. Thin section observations at the northern margin of the Rice Lake batholith revealed a flattening deformation of the granitoid rocks with only minor indications for shear.

IMPLICATIONS FOR THE REGIONAL DEVELOPMENT OF THE SWAYZE AND ABITIBI GREENSTONE BELTS

Since the different lithotectonic assemblages of the Abitibi granite-greenstone belt, including the Swayze portion are correlative and indicate coeval development, models for the overall genesis and evolution of the Abitibi belt must explain the features evident in the Swayze portion of the Abitibi greenstone belt as well. Different models have been proposed for the overall genesis and evolution of the Abitibi greenstone belt. Hodgson (1986) suggested that the southern Abitibi greenstone belt developed on pre-existing crust during extensive rifting and mantle diapirism. However, none of these models is able to explain all the different aspects of the southern Abitibi greenstone belt (Thurston 1991). It is now generally agreed that the evolution of the Abitibi greenstone belt in some form resembles that of an island arc (Thurston 1991). Three different island-arc models have been proposed (e.g., Dimroth et al. 1983; Hodgson and Hamilton 1989; Ludden et al. 1986) that differ dramatically in detail.

Dimroth et al. (1983) suggested an island-arc model for the Abitibi belt that includes a north-dipping subduction zone. Evidence for this subduction is visible in seismic profiles of the Abitibi belt (Bellefleur et al. 1998). In their model, the ultramafic to mafic volcanic rocks are interpreted to represent oceanic crust accreted to the calc-alkalic volcanic rocks representing island arcs. Large volumes of granitoid material were intruded into this pre-existing crust and led to uplift and erosion of the arc complex. This resulted in the development of a sedimentary basin south of the island arcs. In their model, the Pontiac Subprovince was, in part, overthrust by the island-arc assemblages during north-south oriented compression that lead to the formation of the now dominant east-west folds.

Ludden et al. (1986) describe the southern Abitibi belt to have formed after a period of intrusion of calc-alkalic volcanic rocks (~2715 Ma) in a continental-arc environment. Rifting of this early arc resulted in rift basins in which the volcanic rocks and sediments were deposited. They also suggested that the northern part of the Abitibi greenstone belt is older than the southern part and that the northern part mainly evolved during emergent volcanism. During a final orogenic phase, the Kenoran orogeny, the northern and southern Abitibi granite-greenstone belts were strongly deformed during a north-south compression, accounting for the present complexity of the belt.

Hodgson and Hamilton (1989) expanded the model of Dimroth et al. (1983). In their model, the northward subduction led to the collision of island arcs with the foreland basin of a continental mass (now the Pontiac Subprovince). The sediments of the Timiskaming assemblage developed from molasse deposits in this collision zone.

All of the above described models include some kind of island-arc assemblage that, in its final stages, collided with a pre-existing or coevally developing crust—the Pontiac Subprovince. None of these models accounts for the earlier east-west shortening that led to the observed north-south trending folds common at least in the Swayze portion of the Abitibi granite-greenstone belt and the northern part of the Abitibi greenstone belt. Bellefleur et al. (1998) report reflectors striking north to northeast, dipping east to southeast with approximately 15° under the Lake Abitibi batholith. They interpret these as lateral shear zones developed to accommodate the north-south shortening.

From new ages and a revised system of lithotectonic assemblages for the southern portion of the Abitibi greenstone belt, Ayer et al. (2002a) and Sproule et al. (2002) conclude that at least some of the volcanic rocks of this area show geochemical affinities to a mantle plume (mainly the komatiites and tholeiitic basalts), whereas others show geochemical signatures that are subduction related. A mantle plume would greatly enhance the uplift that, according to Dimroth et al. (1983), must have occurred due to the introduction of large volumes of granitoid material to the base of the crust. Timing between the processes of subduction and the rise of a mantle plume is critical and has not yet been fully understood. It seems clear from geochemical analyses (Sproule et al. 2002) that some of the komatiites derive from a plume head, whereas others derive from the tail of the plume (Sproule et al. 2002). Multiple cycles of this komatiite deposition can be observed in the Abitibi belt. No exact geochronological data for these cycles have been published yet. However, the komatiites in the Abitibi greenstone belt are restricted to the Pacaud assemblage (2750–2735 Ma), the Stoughton–Roquemaure assemblage (2723–2720 Ma), the Kidd–Munro assemblage (2719–2710 Ma) and the Tisdale assemblage (2710–2703 Ma) (Sproule et al. 2002), whereas, in the Swayze portion of the Abitibi granite-greenstone belt, komatiites can only be found in the Kidd–Munro assemblage in the north and the Swayze group in the central part (reported ages range between 2702 and 2705 Ma, Heather and Shore 1999). It appears that between the deposition of the tail-related komatiites and head-related komatiites, or in other words, the time span between the cessation of a mantle plume and the arrival of a new one (if there was more than one), there is not enough time to complete a full subduction process. This suggests that plume activity was coeval with, and in close spatial relationship to, subduction.

Acknowledgments

J.K. Becker thanks the German Research Foundation (DFG) for support through the grant BE2101/3-1, and additional support under an Ontario Geological Survey–University of Ottawa Collaborative Project Agreement.

Appendix 1

Data from the AMS Measurements

Appendix 1. Data from the AMS measurements (calculated averages from each site).

Out-crop	UTM 17T Easting	UTM 17T Northing	Susc. ($\times 10^{-6}$ SI)	K1-strike	K1-dip	K2-strike	K2-dip	K3-strike	K3-dip	P'	T
A89	420091	5285943	4592	113	5	204	11	357	78	1.417	0.544
A90	420087	5287791	454	113	8	205	14	353	74	1.039	0.050
A91	420427	5288114	240	109	11	12	33	215	54	1.032	-0.527
A92	420489	5287150	1824	125	36	30	7	290	53	1.214	0.328
A95	421909	5286454	16896	143	37	44	12	299	51	1.627	-0.323
A96	421758	5285756	602	145	41	278	39	30	26	1.627	-0.011
A97	421273	5287261	352	156	41	287	37	40	27	1.070	0.137
A99	423558	5284681	2739	154	26	248	9	356	62	1.264	-0.602
A100	422751	5284752	3247	136	19	232	18	3	63	1.264	0.428
A101	422091	5283999	2387	114	8	24	3	270	82	1.247	-0.334
A102	22023	5282766	563	151	44	325	46	58	3	1.058	-0.651
A103	421550	5282472	498	145	63	277	19	13	19	1.048	0.503
A104	421022	5283877	543	159	39	26	41	272	26	1.346	-0.338
A106	413936	5304369	8573	298	53	153	32	52	17	1.152	0.560
A107	411985	5307047	6717	169	7	1	82	259	2	1.122	0.477
A108	411085	5305149	34004	149	2	58	19	245	71	1.038	-0.590
A109	411596	5303291	1286	303	55	140	33	45	8	1.347	0.489
A110	411270	5301927	2286	155	69	302	18	35	11	1.208	0.239
A119	409909	5304230	559	329	61	158	29	66	4	1.401	-0.096
A123	412859	5312348	2402	249	51	359	16	101	35	1.197	-0.396
A124	412201	5313679	5523	250	41	140	22	29	41	1.271	0.237
A125	411565	5310061	4301	236	40	333	8	73	49	1.154	-0.170
A126	416759	5326441	341	284	37	192	3	98	53	1.115	-0.176
A129	417312	5326321	463	237	17	339	35	125	50	1.117	0.480
A130	416930	5322223	28521	36	14	300	21	156	64	1.036	0.825
A131	417038	5323129	1100	262	20	168	10	52	68	1.178	0.001
A133	416258	5321498	2566	251	14	151	35	359	52	1.176	-0.064
A134	414573	5320426	1374	249	12	156	18	12	68	1.096	-0.487
A135	411055	5319295	458	241	12	149	10	21	74	1.102	-0.070
A136	409025	5320289	213	241	24	347	32	122	48	1.161	0.518
A138	407625	5315654	1199	62	7	330	20	170	68	1.255	0.711
A139	407563	5312407	240	187	56	67	19	326	27	1.241	-0.316
A145	406379	5313324	279	199	34	108	3	14	56	1.245	0.085
A146	407799	5314334	189	164	29	266	21	27	53	1.038	0.151
A148	429832	5328920	145	302	22	64	53	199	28	1.317	0.781
A149	428475	5327546	709	302	17	200	34	53	50	1.282	-0.257
A150	426745	5326737	598	286	20	146	65	21	15	1.206	0.132
A151	426417	5324796	34278	322	36	104	47	217	20	1.412	0.080
A152	426012	5323040	8032	305	17	91	69	212	11	1.102	-0.027
A153	426402	5320890	7243	122	15	221	31	9	55	1.101	0.475
A154	424460	5317654	8898	268	62	122	24	26	14	1.090	0.717
A155	422537	5316078	1515	238	54	22	30	122	17	1.244	-0.421
A156	407022	5315186	163	3	17	261	33	116	51	1.147	0.904
A161	418983	5316141	2050	55	14	150	19	291	66	1.045	0.471

Appendix 1. Continued

Out-crop	UTM 17T Easting	UTM 17T Northing	Susc. ($\times 10^{-6}$ SI)	K1-strike	K1-dip	K2-strike	K2-dip	K3-strike	K3-dip	P′	T
A162	421561	5314904	916	359	13	268	3	167	76	1.043	0.475
A163	423473	5314384	3065	285	4	193	27	23	62	1.149	0.068
A164	423540	5309804	8395	268	37	2	6	100	52	1.212	0.014
A165	425332	5311071	1169	307	52	180	25	77	26	1.110	0.167
A166	424944	5315612	10355	277	36	177	13	71	51	1.055	-0.383
A169	428335	5313527	3300	238	17	116	59	336	25	1.047	-0.037
A170	426537	5319760	3749	303	34	96	53	204	13	1.120	0.743
A174	435695	5342996	320	348	73	95	5	187	16	1.168	0.575
A176	440253	5345768	4236	249	16	136	53	350	32	1.176	-0.448
A179	446392	5351587	5577	263	17	11	45	158	40	1.131	-0.612
A182	457287	5345898	178	292	5	200	16	38	73	1.147	-0.128
A183	457000	5337800	1379	42	17	310	17	200	71	1.250	-0.580
A184	450977	5336542	35001	357	4	218	85	87	4	1.037	0.524
A185	456033	5328121	60558	176	20	338	69	84	6	1.045	0.135
23	414261	5298128	1864	90	46	246	41	347	12	1.111	-0.029
24	413012	5298024	205	112	70	265	18	358	8	1.043	0.033
25	412065	5297877	21871	230	70	56	19	325	2	1.223	-0.177
27	411837	5296794	560	23	15	118	18	256	67	1.466	-0.992
28	411715	5296284	6634	75	40	295	43	184	22	1.172	0.180
29	411475	5295861	5731	15	74	258	7	167	14	1.341	0.790
30	410302	5295424	2694	8	76	266	3	175	13	1.229	0.217
31	410271	5294411	3451	339	60	90	12	186	27	1.111	0.254
32	409565	5293646	41500	145	17	241	20	17	64	1.054	-0.615
33	408987	5293145	19698	71	64	205	19	301	17	1.396	0.248
34	406936	5290592	17438	108	55	9	6	274	34	1.198	0.033
35	406402	5291538	1672	264	84	26	5	116	4	1.017	-0.439
36	406018	5292286	1360	264	45	54	41	158	16	2.061	-0.857
37	405310	5293245	144	93	5	195	69	1	21	1.016	-0.275
38	408556	5292370	449	181	3	90	5	299	85	1.007	-0.343
39	408550	5291488	112	231	55	42	34	135	4	1.007	-0.400
40	407342	5290852	40887	174	52	278	11	16	36	1.132	0.471
44	409055	5290135	134483	27	23	149	51	283	30	1.274	0.818
45	406966	5290321	14746	287	9	197	3	92	80	1.672	-0.560
46	410197	5292604	3269	229	34	81	51	330	16	1.153	0.273
47	409915	5292397	44824	153	0	63	6	245	84	1.047	0.425
48	410342	5290344	1199	192	31	91	17	336	53	1.016	0.827
52	411778	5279861	8201	136	12	230	16	13	70	1.384	0.527
53	411233	5280178	9675	143	4	235	24	43	66	1.686	0.670
58	422051	5276025	2378	105	7	205	54	9	35	1.242	0.690
60	416007	5289307	40173	278	14	182	19	42	66	1.143	-0.614
63	415898	5287611	7067	13	7	128	73	281	15	1.612	-0.746
64	415336	5288005	463	229	43	338	20	86	41	1.020	0.791
66	414917	5286492	463	253	26	356	25	124	53	1.032	0.374
67	414097	5285845	482	305	41	204	13	100	46	1.064	-0.049

Appendix 1. Continued

Out-crop	UTM 17T Easting	UTM 17T Northing	Susc. ($\times 10^{-6}$ SI)	K1-strike	K1-dip	K2-strike	K2-dip	K3-strike	K3-dip	P′	T
68	414222	5284503	7308	268	28	167	19	47	55	1.682	0.474
69	414127	5283022	652	293	33	172	39	49	34	1.112	0.427
70	414888	5289428	450	296	22	194	26	61	55	1.030	0.495
71	414409	5288526	609	271	33	170	17	56	52	1.212	-0.019
73	413367	5286396	136110	323	37	222	14	116	50	1.456	0.345
74	413491	5284869	19805	268	42	29	30	141	33	1.306	-0.632
75	413250	5283791	526	288	37	24	8	125	52	1.039	0.221
76	413325	5281741	11199	246	30	154	3	59	60	1.497	0.896
77	413275	5280904	20766	146	18	40	41	254	43	1.242	-0.089
78	413194	5280373	13850	163	31	270	27	33	47	1.800	0.925
79	413490	5277837	5086	135	22	235	22	5	58	1.324	0.015
80	414074	5278607	8797	134	9	230	33	32	55	1.453	0.507
81	414177	5279445	2169	122	28	330	59	219	12	1.187	-0.290
82	414734	5279599	11840	212	21	117	12	359	65	1.776	0.856
83	414425	5280819	13309	276	25	176	21	51	56	1.647	0.769
84	414691	5281767	4104	263	40	167	7	69	49	1.862	0.502
85	415418	5282969	1436	277	32	13	9	117	57	1.106	0.438
86	415646	5283980	543	291	30	187	22	67	51	1.063	0.427
87	416053	5284438	4220	294	23	184	39	47	42	1.355	0.160
88	417245	5285156	13332	294	5	200	45	29	44	1.172	0.414
89	417730	5283822	3555	284	10	193	7	69	78	1.154	-0.540
90	418021	5282950	4459	280	23	138	61	17	16	1.318	-0.141
91	418113	5281926	538	289	1	198	37	20	53	1.043	0.074
92	418303	5282982	5941	296	16	184	52	37	33	1.162	0.359
94	415820	5281848	339	248	55	103	30	3	17	1.054	0.073
95	416596	5280683	3365	242	47	337	4	70	43	1.126	-0.132
96	416772	5281722	2518	127	1	218	25	34	65	1.683	0.513
97	417896	5280740	11772	307	30	174	50	52	25	1.339	0.097
99	418145	5278011	10472	103	7	201	51	8	38	1.405	0.539
100	418670	5277471	230	263	14	165	29	16	57	1.075	0.971
101	417308	5278120	1457	234	44	132	12	30	43	1.190	0.587
103	416678	5278423	3387	273	10	178	26	21	62	1.790	0.767
104	417464	5279070	554	284	21	185	22	53	59	1.046	0.738
105	417674	5279982	4098	307	11	207	44	48	44	1.346	0.302
108	416621	5293822	2449	267	35	56	51	166	15	1.270	-0.622
112	416353	5290425	3044	105	22	10	14	248	64	1.186	-0.543
114	416041	5289347		263	69	97	20	5	5	1.393	0.230
188	417478	5294039	5786	291	37	141	49	33	15	1.374	-0.796
199	417644	5295505	19701	125	43	305	47	215	0	1.657	0.891
201	418058	5294484	91	145	3	254	81	54	9	1.168	0.870
203	421901	5300171	2451	13	52	278	3	185	38	1.040	-0.306
204	422928	5299552	1336	244	10	146	38	346	50	1.306	0.448

References

Ayer, J.A., Amelin, Y., Corfu, F., Kamo, S., Ketchum, J., Kwok, K. and Trowell, N. 2002a. Evolution of the southern Abitibi greenstone belt based on U-Pb geochronology: autochthonous volcanic construction followed by plutonism, regional deformatoin and sedimentation; Precambrian Research, v.115, p.63-95.

Ayer, J.A., Ketchum, J.W.F. and Trowell, N.F. 2002b. New geochronological and Nd isotopic results from the Abitibi greenstone belt, with emphasis on timing and tectonic implications of Late Archean sedimentation and volcanism; *in* Summary of Field Work and Other Activities 2002, Ontario Geological Survey, Open File Report 6100, p.5-1 to 5-16.

Barker, F. and Arth, J.G. 1976. Generation of trondhjemitic-tonalitic liquids and Archean bimodal trondhjemite-basalt suites; Geology, v.4, p.596-600.

Becker, J.K., Siegesmund S. and Jelsma H.A. 2000. The Chinamora batholith, Zimbabwe: structure and emplacement related magnetic rock fabric; Journal of Structural Geology, v.22, p.1837-1853.

Bellefleur, G., Calvert, A.J. and Chouteau, M.C. 1998. Crustal geometry of the Abitibi Subprovince, in light of three-dimensional seismic reflector orientations; Canadian Journal of Earth Sciences, v.35, p.569-582.

Borradaile, G. and Craig, A., 1987. Relationship between magnetic susceptibility and strain in laboratory experiments; Tectontophysics, v.133, p.121-135.

Bouchez, J.L., Delas, C., Gleizes, G. and Nédélec, A. 1992. Submagmatic microfractures in granites; Geology, v.20, p.35-38.

Dimroth, E., Imreh, L., Goulet, N. and Rocheleau, M. 1983. Evolution of the south-central segment of the Abitibi greenstone belt, Quebec. Part III: Plutonic and metamorphic evolution and geotectonic model; Canadian Journal of Earth Sciences, v.20, p.1374-1388.

Feng, R. and Kerrich, R. 1992. Geochemical evolution of granitoids from the Archean Abitibi southern volcanic zone and the Pontiac subprovince, Superior Province, Canada: implications for tectonic history and source regions; Chemical Geology, v.98, p.23-70.

Foerster, H.J., Tischendorf, G. and Trumbull, R.B. 1997. An evaluation of the Rb vs. (Y+Nb) discrimination diagram to infer tectonic setting of silicic igneous origin; Lithos, v.40, p.261-293.

Hall, L.A.F. 2001. Geology and mineral potential of Carscallen and Denton townships, Timmins west area; *in* Summary of Field Work and Other Activities 2001, Ontario Geological Survey, Open File Report 6070, p.5-1 to 5-11.

Heather, K.B. 1998. New insights on the stratigraphy and structural geology of the southwestern Abitibi greenstone belt: Implications for the tectonic evolution and setting of mineral deposits in the Superior Province; abstract *in* Program, Prospectors and Developers Association of Canada, Annual Convention and Trade Show, Toronto, Ontario.

Heather, K.B. and van Breemen, O. 1994. An interim report on geological, structural, and geochronological investigations of granitoid rocks in the vicinity of the Swayze greenstone belt, southern Superior Province, Ontario, Canadian Shield; *in* Current Research, Part C, Geological Survey of Canada, Paper 1994-C, p.259-268.

Heather, K.B. and Shore, G.T. 1999. Geology, Swayze greenstone belt, Ontario; Geological Survey of Canada, Open File 3384a-i, scale 1:50 000.

Heather, K.B., Shore, G.T. and van Breemen, O. 1995. The convoluted "layer-cake", an old recipe with new ingredients for the Swayze greenstone belt, southern Superior Province, Ontario; *in* Current Research, Part C, Geological Survey of Canada, Paper 1995-C, p.1-10.

——— 1996. Geological investigations in the Swayze greenstone belt, southern Superior Province, Ontario; a final field update, Canadian Shield; *in* Current Research, Part C, Geological Survey of Canada, Paper 1996-C, p.125-136.

Hodgson, C.J. 1986. Abitibi greenstone belt, Ontario, Canada; Transactions of the Institution of Mining and Metallurgy, v.95, p.B183-B194.

Hodgson, C.J. and Hamilton, J.V. 1989. Gold mineralization in the Abitibi greenstone belt; end-stage results of Archean collisional tectonis?; *in* The geology of gold deposits; the perspective in 1988, Economic Geology Monograph 6, p.86-100.

Jelinek, V. 1981. Characterization of magnetic fabric of rocks; Tectonophysics, v.79, p.563-567.

Ludden, J., Hubert, C. and Gariepy, C. 1986. The tectonic evolution of the Abitibi greenstone belt of Canada; Geological Magazine, v.123, pt.2, p.153-166.

Milne, V.G. 1972. Geology of the Kukatush–Sewell lakes area; District of Sudbury; Ontario Geological Survey, Report 97, 116p.

Pearce, J.A., Harris, N.B.W. and Tindle, A.G. 1984. Trace element discrimination diagrams for the tectonic interpretation of granitic rocks; Journal of Petrology, v.25, p.956-983.

Siegesmund, S., Jelsma, H.A., Becker, J.K., Davies, G., Layer, P., van Dijk, E., Kater, L. and Vinyu, M. 2002. Constraints on the timing of granite emplacement, deformation and metamorphism in the Shamva area, Zimbabwe; International Journal of Earth Sciences, v.91, p.20-34.

Sproule, R.A., Lesher, C.M., Ayer, J.A., Thurston, P.C. and Herzberg, C.T. 2002. Spatial and temporal variations in the geochemistry of komatiites and komatiitic basalts in the Abitibi greenstone belt; Precambrian Research, v.115, p.153-186.

Tarling, D.H. and Hrouda, F. 1993. The magnetic anisotropy of rocks; Chapman and Hall, London, 217p.

Thurston, P.C. 1991. Archean geology of Ontario: Introduction; *in* Geology of Ontario, Ontario Geological Survey, Special Volume 4, Part 1, p.73-78.

Metric Conversion Table

Conversion from SI to Imperial			Conversion from Imperial to SI		
SI Unit	*Multiplied by*	*Gives*	*Imperial Unit*	*Multiplied by*	*Gives*
		LENGTH			
1 mm	0.039 37	inches	1 inch	**25.4**	mm
1 cm	0.393 70	inches	1 inch	**2.54**	cm
1 m	3.280 84	feet	1 foot	**0.304 8**	m
1 m	0.049 709	chains	1 chain	20.116 8	m
1 km	0.621 371	miles (statute)	1 mile (statute)	**1.609 344**	km
		AREA			
1 cm^2	0.155 0	square inches	1 square inch	**6.451 6**	cm^2
1 m^2	10.763 9	square feet	1 square foot	**0.092 903 04**	m^2
1 km^2	0.386 10	square miles	1 square mile	2.589 988	km^2
1 ha	2.471 054	acres	1 acre	0.404 685 6	ha
		VOLUME			
1 cm^3	0.061 023	cubic inches	1 cubic inch	**16.387 064**	cm^3
1 m^3	35.314 7	cubic feet	1 cubic foot	0.028 316 85	m^3
1 m^3	1.307 951	cubic yards	1 cubic yard	0.764 554 86	m^3
		CAPACITY			
1 L	1.759 755	pints	1 pint	0.568 261	L
1 L	0.879 877	quarts	1 quart	1.136 522	L
1 L	0.219 969	gallons	1 gallon	**4.546 090**	L
		MASS			
1 g	0.035 273 962	ounces (avdp)	1 ounce (avdp)	28.349 523	g
1 g	0.032 150 747	ounces (troy)	1 ounce (troy)	**31.103 476 8**	g
1 kg	2.204 622 6	pounds (avdp)	1 pound (avdp)	**0.453 592 37**	kg
1 kg	0.001 102 3	tons (short)	1 ton (short)	**907.184 74**	kg
1 t	1.102 311 3	tons (short)	1 ton (short)	**0.907 184 74**	t
1 kg	0.000 984 21	tons (long)	1 ton (long)	**1016.046 908 8**	kg
1 t	0.984 206 5	tons (long)	1 ton (long)	**1.016 046 90**	t
		CONCENTRATION			
1 g/t	0.029 166 6	ounce (troy)/ ton (short)	1 ounce (troy)/ ton (short)	34.285 714 2	g/t
1 g/t	0.583 333 33	pennyweights/ ton (short)	1 pennyweight/ ton (short)	1.714 285 7	g/t

OTHER USEFUL CONVERSION FACTORS

	Multiplied by	
1 ounce (troy) per ton (short)	31.103 477	grams per ton (short)
1 gram per ton (short)	0.032 151	ounces (troy) per ton (short)
1 ounce (troy) per ton (short)	20.0	pennyweights per ton (short)
1 pennyweight per ton (short)	0.05	ounces (troy) per ton (short)

Note: Conversion factors which are in bold type are exact. The conversion factors have been taken from or have been derived from factors given in the Metric Practice Guide for the Canadian Mining and Metallurgical Industries, published by the Mining Association of Canada in co-operation with the Coal Association of Canada.

ISSN 0826-9580
ISBN 0-7794-4430-2